Freie Universität Berlin

Polyvalent Virus Inhibitors Based on Functionalized Carbon Nanoarchitectures

DISSERTATION

zur Erlangung des akademischen Grades des

Dokotors der Naturwissenschaften (Dr. rer. nat.)

eingereicht im Fachbereich Biologie, Chemie, Pharmazie

der Freien Universität Berlin

vorgelegt von

Benjamin Ziem

aus Berlin

November 2016

Diese Arbeit wurde unter Anleitung von Prof. Dr. Rainer Haag im Zeitraum von Juni 2012 bis November 2016 am Institut für Chemie und Biochemie der Freien Universität Berlin angefertigt.

1. Gutachter: Prof. Dr. Rainer Haag, Freie Universität Berlin

2. Gutachter: Prof. Dr. Mohsen Adeli, Lorestan University

Disputation am 16. Dezember 2016

I hereby declare that this PhD thesis entitled “Polyvalent virus inhibitors based on functionalized carbon nanoarchitectures” is the result of my own research and that all utilized sources and references are acknowledged properly by referring to the original work.

Benjamin Ziem
Berlin, 28.11.2016

Dedicated to my wife Nora
and my daughter Lotta

Eines der wunderbarsten Geschenke ist Zeit,
doch nur die Wenigsten wissen sie rechtzeitig zu schätzen.

Acknowledgements

First of all, I would like to thank Prof. Dr. Rainer Haag for giving me the opportunity to be a part of his group, his great confidence and his financial as well as scientific support over the last years.

Secondly, I would like to thank Prof. Dr. Mohsen Adeli for being my second reviewer, the open and friendly conversations, and the fruitful collaboration.

Furthermore, I would like to thank all my cooperation partners in no particular order for great support and helpful discussions: Mohammad Fardin Gholami, Hendrik Thien, Ievgen Donskyi, Kim Silberreis, Dr. Fabian Beckert, Dr. Katharina Achazi, Dr. Constanze Yue, Dr. Daniel Stern, Dr. Dominic Gröger, Dr. Jessica Rahn, Dr. Walid Azab, Dr. Luis Cuellar, Dr. Jens Dernedde, PD Dr. Andreas Nitsche, Prof. Dr. Jürgen P. Rabe, Prof. Dr. Thomas C. Mettenleiter, Prof. Dr. Nikolaus Osterrieder, and Prof. Dr. Rolf Mülhaupt.

I also would like to thank all present and past group members of the AG Haag for the friendly atmosphere and a great time. Especially, Mathias Dimde, Sabine Reimann, Virginia Wycisk, Nadine Rades, Karolina Walker, Dr. Jonathan Vonnemann, Dr. Pradip Dey, Dr. Florian Paulus, Dr. Dirk Steinhilber, Dr. Emanuel Fleige, Dr. Indah Nurita Kuniasih, Dr. Katja Neuthe, Dr. Carlo Fasting, Dr. Sumati Bhatia, Dr. Marie Weinhart, and Dr. Qiang Wei. Further, I would like to thank my former fellow students Ina Halfpap, Dr. Emanuel Hupf, Dr. Carsten Lüdtke, and Dr. Darina Heinrich for the wonderful but not always easy time together.

A special thanks goes to Dr. Wiebke Fischer for her great support and her kindness. Furthermore, I would like to thank Jutta Hass and Dr. Pamela Winchester for helping me with bureaucratic hurdles, proofreading, and for the nice conversations. I wish both a relaxing retirement and many wonderful moments with their families. I also want to acknowledge the analytical department at the FU Berlin for their kind support and the whole AG Böttcher for pleasant and fruitful discussion.

Finally I want to thank my family and friends for all the support, understanding, patience, and trust throughout my education and my entire life. But the greatest thanks for simply everything go to my beloved wife Nora and my little Chaos queen Lotta.

Contents

1. Introduction

All natural or synthetic materials ranging from 1 nm up to 1000 nm in size such as proteins, viruses, or even inorganic particles like quantum dots and carbon allotropes (e.g. fullerenes, nanotubes, graphene) can be defined as nanomaterials. The interest for these materials has increased exponentially over the last decades in most scientific areas, especially in the fields of nanomedicine,[1] electronics,[2] and cosmetics.[3] This is mainly due to the fact that most of this materials exhibit unique physicochemical properties that can be further modified by various functionalizations. Carbon-based nanostructures, for example, show interesting properties such as magnetism, electrical conductivity, as well as optical properties, depending on the size, shape and particularly the chemical structure.[4] Furthermore, these materials provide large surface areas, which can be used as tuneable scaffolds for small molecules, bioactive ligands, drugs, and targeting moieties to achieve polyvalent hybrid-nanoarchitectures. These could be the key elements, especially in the field of nanomedicine, for developing new urgently needed pathogen inhibitors to fight viruses and bacteria, which are known to strongly adhere to cells by multivalent binding.[5, 6] Most pathogens exhibiting large contact areas and multiple receptor sites, due to their sizes ranging from several nanometers up to micrometer scale. For this reason, there is a strong need for polyvalent architectures that have pathogen- or cell-like dimensions.

The main focus in this work is the development of novel nanoarchitectures by combining especially thermally reduced graphene oxide (TRGO) with the biological active polyglycerol sulfate (PGS) to generate potent inhibitors for heparan sulfate dependent viruses. dPGS is already known to be an efficient entity which targets inflammatory diseases and has the potential to inhibit viral infections.[7-10] Furthermore, it represents a synthetic analog of heparin, which is in many cases the standard therapeutic in the field of medical treatment for inflammatory diseases.[7, 11] However, the small size (2-20 nm) and the spherical shape of dPGS are limiting factors for a potential inhibition. For this reason, different scaffold materials are used to adapt size of dPGS to pathogen-like dimensions.

In this thesis, the graphene-based hybrid-nanoarchitectures are used as model system which was systematically varied in the degree of sulfation, the polymer loading, the sheet size, and the used polymer to evaluate the impact of these parameters on the inhibition efficacy. Additionally, further functionalized nanomaterials have been developed by combining dPGS with nanodiamonds, carbon nanotubes, and fullerenes to gain extra information that could be relevant for prospective inhibitor designs.

1.1 Carbon-based nanomaterials

1.1.1 Graphite / Graphene

Graphite is a multilayer carbon-based material that has already been known since the artisans of Thrace and Macedonia used it for painting their ceramics at the end of the Late Neolithic period.[12] But after its discovery, it took an additional 4000 years to break down this mineral into the monolayer level. The so-called graphene was isolated the first time by Geim and Novoselov, who were awarded with the Nobel prize in 2010 for this. Graphene is a slightly wrinkled, honeycomb-like monolayer sheet based on a two-dimensional (2D) arrangement of sp^2-hybridized carbon atoms.[13-15] Because of its high flexibility, it can be seen as a building block for setting up differently dimensional carbon structures like fullerenes (0D), nanotubes (1D), or the mineral graphite (3D).[15]

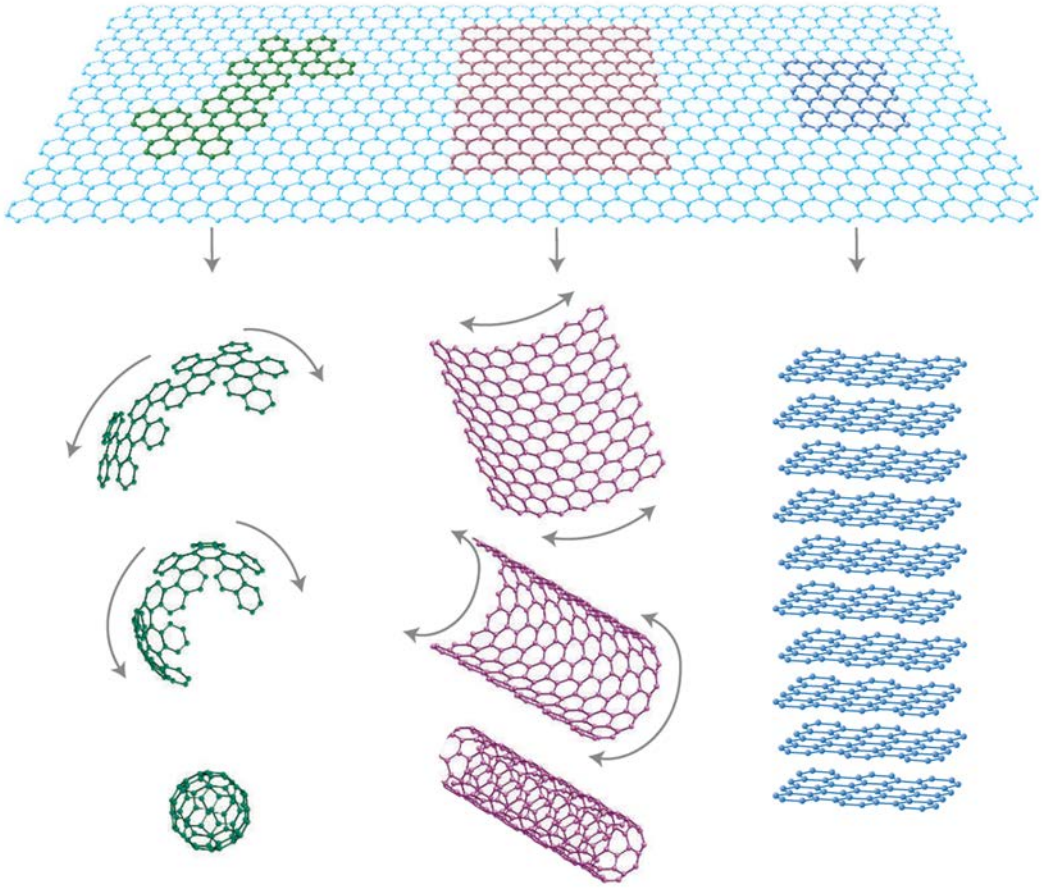

Figure 1. Mother of all graphitic forms. Graphene is a 2D building material for carbon materials of all other dimensionalities. It can be wrapped up into 0D buckyballs, rolled into 1D nanotubes or stacked into 3D graphite. Reproduced with permission from Ref.15, Copyright 2007, Nature Publishing Group.

Graphene's very special physical properties like high mechanical flexibility, optical transparency, as well as excellent electrical and thermal conductivity make ite an unique

material, one which has aroused enormous interest in nearly all fields of science over the last decade.[13-20] Additionally, it offers a huge surface area of approximately 2600 m^2/g, which can be functionalized or modified further to pave the way for new fields of application such as filtration, detection or inhibition in healthcare and environmental protection.

However, the production of graphene is still challenging, especially on a large scale. For this reason, different methods have been invented that range from direct exfoliation of natural graphite, unzipping of carbon nanotubes, chemical vapor deposition (CVD) to chemical or thermal reduction of graphite oxide (GO).[21, 22] All the enumerated methods have their assets and drawbacks, particularly regarding their economic efficiency and scalability. Therefore the fabrication of graphene starting from GO is one of the most frequently and convenient procedures worldwide.

1.1.2 Graphite oxide

The first synthesis of graphite oxide relates back to the work of Benjamin C. Brodie in 1855 who oxidized pristine graphite flakes under harsh conditions.[23] The major drawback in this method is that it exposes the highly explosive gas chlorine dioxide. For this reason, various methods have been developed over the last 160 years, but the most famous and many times modified procedures are still the oxidation methods of Brodie, Staudenmaier,[24] as well as Hummers and Offeman.[25] Out of this three preparations the oxidation by Hummers and Offeman is the most convenient one and has the lowest risk during the reaction. In short, pristine graphite flakes are oxidized by a mixture of concentrated sulfuric acid and potassium permanganate below 45°C.

However, independently of the used oxidation method, the layer distance within the graphite structure doubled from 0.34 nm to ~0.70 nm due to the insertion of different functional groups. Scientists are still not 100% clear about the exact structure of the GO. Although several structural models were proposed in the last century, research is still ongoing in this field. In one of the first models Hofmann and Holst in 1939 indicated the presence of hydroxyl and carboxyl groups.[26] Today the most accepted structural model is derived from studies by Lerf and Klinowski.[27] They showed that GO is a highly oxidized, nearly amorphous material with different stoichiometries depending on the fabrication method as well as graphite source. Nevertheless, the structure can be described as a surface that exhibits hydroxyls, epoxides, ketones, and diols on the basal plains while carbonyl as well as carboxyl groups are located at the edges. Even if GO is considered as nearly

amorphous material, the suggested stoichiometry ($C_6H_2O_3$) by Boehm and co-workers for Hummers compounded graphite oxide is widely accepted.[28]

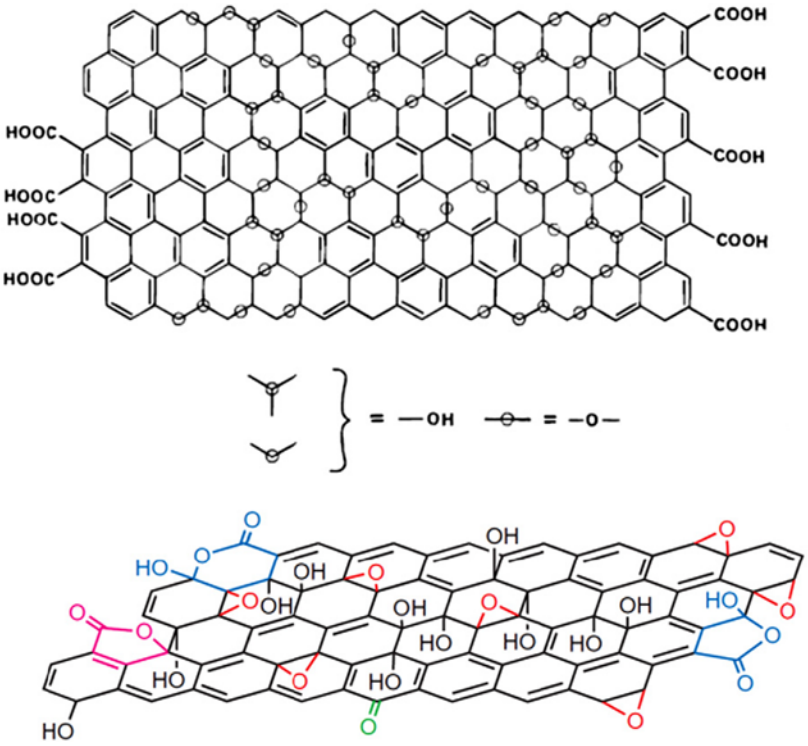

Figure 2. Structural models of GO by Lerf and Klinowski showing hydroxyl, epoxide, ketone, and diol groups on the basal plains while carbonyl, as well as carboxyl groups, are located at the edges. Reproduced with permission from Ref. 27 (top) Copyright 1998, American Chemical Society and 29 (bottom), Copyright 2009, Nature Publishing Group.

1.1.3 Reduced graphene oxide

Even though there are several ways to obtain few layer or mono-layer graphene as already mentioned in Section 1.1.1, one of the most frequently and convenient methods is to reduce graphite oxide, which can be realized thermally as well as chemically by using a reducing agent such as hydrazine hydrate or borane tetrahydrofuran complex.[30, 31] In the case of a thermal reduction, no further purification steps are required which makes this method superior compared to the chemically done procedure. This method relies on the thermal instability of the graphite oxide that results in an explosive exfoliation at temperatures above 230 °C.[28] The driving force for the massive expansion can be assigned to the spontaneous release of carbon dioxide, carbon monoxide, and water vapor during the reduction of the epoxides, ketones, diols, carbonyls, as well as carboxyl's due to rapid heating.[31, 32] In contrast to the ideal graphene structure, the thermally reduced graphene

oxide (TRGO) does not possess a complete sp^2 hybridization, because many carbon centers are still sp^3-hybridized as a result of the remaining hydroxyl functionalities. These hydroxyl groups are easily accessible and can be used for further functionalizations to develop potent pathogen inhibitors which are the focus of this work.

1.1.4 Fullerenes

In 1985 Smalley and coworkers were able to manufacture the first C_{60} fullerenes by vaporizing graphite using a focused pulse laser.[33] The generated Buckminsterfullerene consists of 60 carbon atoms which are arranged in 12 pentagonal and 20 hexagonal rings forming a football like structure (See Figure 9g). Besides its unique physical and chemical properties,[34] the C_{60} is known to be the most symmetrical molecule possessing 120 symmetrical operations.[35] It is fully sp^2-hybridized like the pristine graphene but it totally differs in its electrical behavior.[36] The fullerene surface can be decorated with various functional groups[37] like amino[38] or carboxylic acids,[39] as well as hydroxyl groups[40] or polymeric ligands,[41] which leads to a wide range of applications. Some of these functionalized buckyballs already have shown good results as antiviral compounds[39] and give hope for future developed fullerene-based virus inhibitors.

1.1.5 Carbon nanotubes

Carbon nanotubes (CNTs) can be described as rolled up graphene sheets (Figure 1) with length dimensions from nanometer up to centimeter size that exhibit unique electronical, mechanical, as well as thermal properties.[42-44] Due to their exceptional characteristics and their large surface area, a broad spectrum of applications are available that range from electronic and materials science to the field of nanomedicine.[45-51] Furthermore, the CNTs can be oxidized under harsh conditions[52-56] similar to the graphene's to obtain primarily hydroxyl and carboxyl functionalities on the graphitic surface. These functional groups can be used for further functionalizations, for example, to enhance the water solubility as well as the biocompatibility and contemporaneously decrease the toxicity.[57, 58] In summary, functionalized CNTs have a tuneable 1D nanoarchitecture which can a high potentially serve in the future as a novel carbon-based pathogen inhibitor, due to their unique physical properties, shape, and size.

1.1.6 Nanodiamonds

In contrast to fullerenes, carbon nanotubes, graphene, and graphite, a nanodiamond (ND) cannot be counted as a graphitic allotrope even if there are graphitic areas in its diamond lattice structure.[59, 60] In general, NDs are produced on an industrial scale by controlled detonations of, for example, mixtures of trinitrotoluene and cyclotrimethylene triamine in a detonation reactor.[61] During the preparation and subsequent purification, a heterogeneous surface is generated, that exhibits various functional groups as shown in Figure 3. The surface mainly bears hydroxyl-, carboxyl-, and keto-groups as well as several lactones, amines, and ethers, which all pave the way beside graphitic areas for different modification methods leading to exceptional characteristics.[62, 63] Nanodiamonds dispose excellent physical and chemical properties such as fluorescence, high hardness, stiffness, and strength as well as good biocompatibility.[64-67]

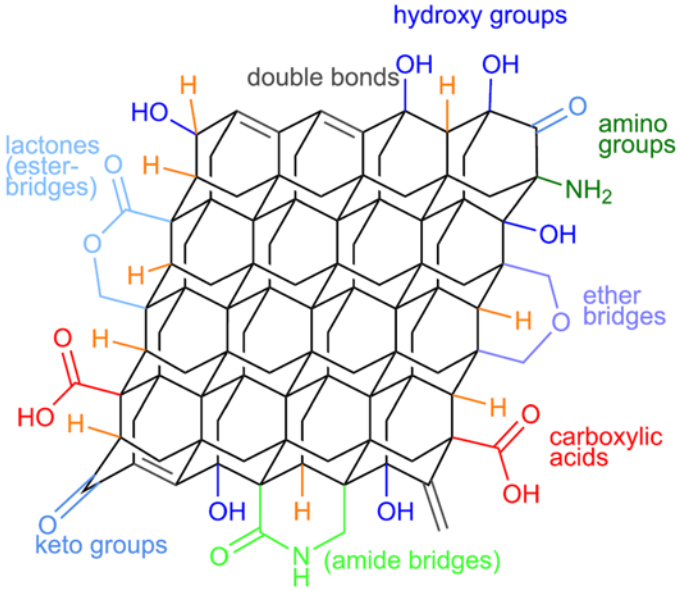

Figure 3. Proposed functional groups on a purified detonation nanodiamond surface. Reproduced under the term of the Creative Commons Attribution License from Ref. 62.

Overall, nanodiamonds are derived from detonation, in the range of 4 - 6 nm in size, almost fully sp^3-hybridized, and thus provide a large surface area up to 420 m^2/g that is decorated with various functional groups for post-modifications.[60, 68, 69] Furthermore, they are well known for their tendency to form aggregates, in particular, dimensions of 100 - 200 nm, 2 - 3 µm, and 20 - 30 µm.[59] This aggregation behavior could be an additional benefit for the development of novel multivalent inhibitors, because the overall system can reach virus- or cell-like dimensions.

1.2 Nature as Source for Inspiration

1.2.1 The multivalency principle

Multivalency can be described as an exceptional and useful principle in nature to control the binding strength and the reversibility in biological processes like self-organization, adhesion, signal transduction, and cell-cell recognition.[6, 70, 71] In general, the principle is based on non-covalent interfacial interactions between *m*-valent ligands and *n*-valent matching receptors ($m, n > 1$; and $m \neq n$).[5] In this connection the overall binding energy of a multivalent architecture is defined by the sum of all monovalent binding events (N) during an interaction process, limited by the contact area between the participants. Due to this concept, nature is able to regulate the binding efficacy of a biological system by varying the size, geometry, ligand/receptor density or by disposal of weaker ligand/receptor pairs.[5, 72-74]

The adhesion process of viruses,[75, 76] bacteria[77, 78] or fungi[79, 80] to a targeted cell is an ideal example for a multivalent interaction as shown below for the influenza virus (Figure 4).[70] The influenza virus exhibits ~ 600 copies of the trimeric hemagglutinin ligands per virus particle,[5] which are all able to interact simultaneously with the sialic acid residues of the cellular glycocalyx.[81] Due to this multivalent adhesion the virus is taken up to the host cell via endocytosis where it subsequently triggers the infection.

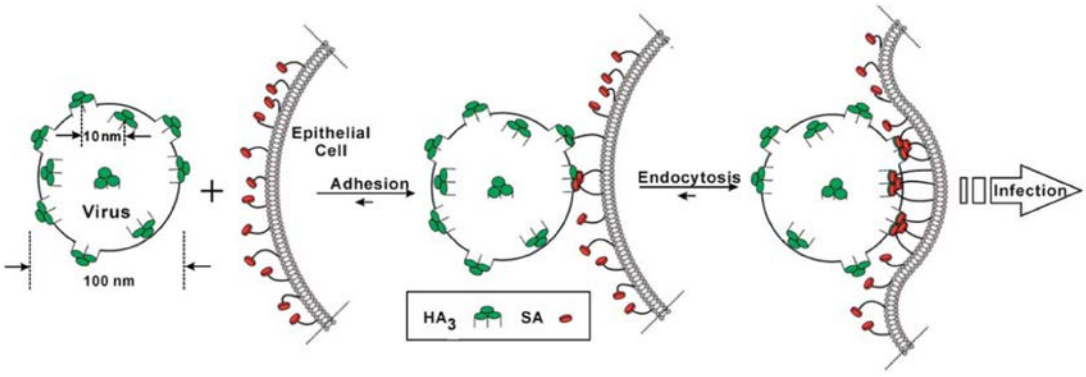

Figure 4. Multivalent interactions between trimeric hemagglutinin (HA_3) on influenza virus and sialic acid (SA) residues on cells leading to endocytosis and infection. Reproduced with permission from Ref. 70, Copyright 2014, The Royal Society of Chemistry.

Even if nature frequently uses the principle of multivalency, the question whether a multivalent binding event is superior to a monovalent analog still has to be answered. Therefore, the thermodynamics needs to be considered especially the change in the free energy ΔG, which is mainly enthalpy driven in case of a monovalent binding and can be

easily explained by the Gibbs equation (Eq. 1), with ΔG defined as binding affinity, ΔH as enthalpic change, and TΔS as temperature-dependent entropic change.

$$\Delta G = \Delta H - T\Delta S \qquad \text{(Eq. 1)}$$

For comparison of the overall binding energy of a monovalent with a multivalent system, it is necessary to use equilibrium constants, since multivalent interactions are more complex and have to be considered as a highly dynamic process. By embedding the cooperativity factor α, it is possible to compare the average binding affinity ΔG_{avg}^{multi} of a multivalent system to its monovalent counterpart ΔG^{mono} (Eq. 2-6).[5] In this connection the used superscripts *mono* and *multi* represent monovalent or multivalent systems exhibiting *N* ligand/receptor pairs and *K* binding constants.

$$\Delta G_{avg}^{multi} = \Delta G_{N}^{multi} / N \qquad \text{(Eq. 2)}$$

$$\Delta G = - RT \ln(K) \qquad \text{(Eq. 3)}$$

$$\Delta G_{avg}^{multi} = \alpha \Delta G^{mono} \qquad \text{(Eq. 4)}$$

$$K_{N}^{multi} = \left(K_{avg}^{multi}\right)^{N} = \left(K^{mono}\right)^{\alpha N} \qquad \text{(Eq. 5)}$$

$$\alpha = \frac{\lg\left(K_{N}^{multi}\right)}{\lg\left(K^{mono}\right)^{N}} \qquad \text{(Eq. 6)}$$

The cooperativity factor α depends on the order of multivalent interaction and can be classified as positively cooperative (synergistic, $\alpha > 1$), non-cooperative (additive, $\alpha = 1$), or negatively cooperative (interfering, $\alpha < 1$).[5, 82] Besides cooperativity, further aspects like stiffness, flexibility of the multivalent system, as well as ligand geometry also influence the overall binding. For this reason, Whitesides[4] and coworkers suggested a simplified interpretation of the binding efficacy expressed by the enhancement factor β, which represents the ratio of binding constants for a multivalent architecture (K^{multi}) and its monovalent analog (K^{mono}).

$$\beta = \frac{K^{multi}}{K^{mono}} \qquad \text{(Eq. 7)}$$

Due to the enhancement factor β, multivalent efficacy can be determined without knowing the exact number of the involved ligand/receptor pairs. Furthermore, it directly includes cooperativity as well as symmetry effects.

1.2.2 Extracellular matrix-inspired inhibitor design

The development of new efficient pathogen inhibitors is a challenging process, since many factors can significantly influence the inhibition efficacy, especially in the case of multivalent systems as discussed in Chapter 1.2.1. The very first step in the development process is to decode the targeted virus or bacterium in order to identify the binding mode and ideally the kinetics behind it. Furthermore, an accurate model[83, 84] of the pathogen surface would be desirable to determine the structure of the receptor as well as their overall distribution. With this information in hand, well target-oriented designs can be developed that exhibit an optimized density of precisely fitting ligands. Meyer[85] and coworkers established a sialic acid-functionalized tripod that fit perfectly on the decoded trimeric hemagglutinin structure,[86-88] which was located all over the influenza virus particle. However, the concept of a perfect 'ligand-receptor conformity' totally depends on the topological decryption of the pathogen and therefore is not applicable for many cases so far.

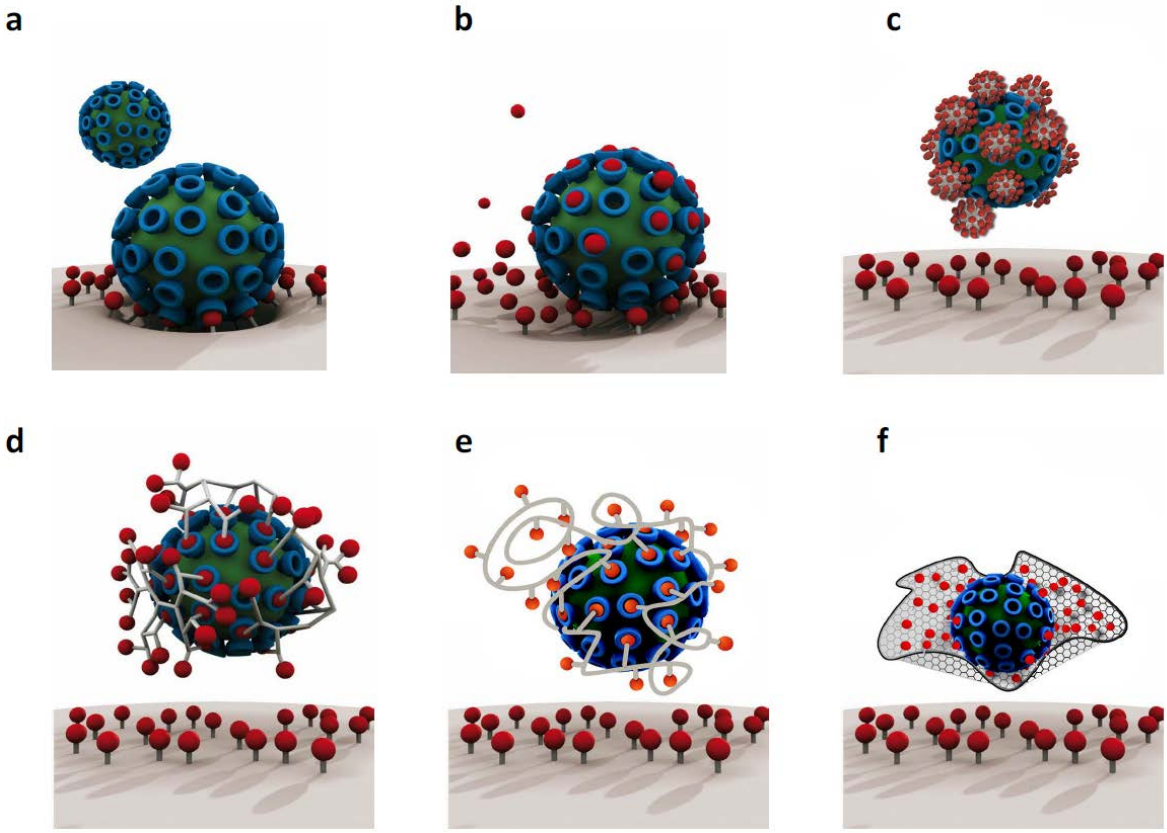

Figure 5. Different approaches for pathogen inhibition. (a) Multivalent interaction of a non-inhibited particle to the cell surface. (b) Particle adhesion to the cell due to an underdose usage of a perfect ligand-receptor inhibitor. (c) Zero-dimensional, spherical, multivalent systems like functionalized nanodiamonds and fullerenes are able to bind to several receptors sites simultaneously and additionally decrease the access for further binding due to their rigidity. (d) Branched and star-like polymer-based architectures can be disposed as highly adaptive inhibitors to enhance the binding and shielding efficacy. (e) A linear polymer can be used as a

highly flexible inhibitor, which can access numerous receptors at the same time and is able to sterically shield further binding sites, due to its fluctuating conformations. (f) A flexible 2D architecture like a functionalized graphene sheet can strongly interact with the pathogen, shield further receptor due to its size, and ideally wrap the whole infectious particle. Figure (a) - (c) are reproduced with permission from Ref. 6, Copyright 2012, John Wiley and Sons, Figure (d) - (f) are reproduced with permission from Ref. 89, Copyright 2016, American Chemical Society.

An alternative concept, which is comparable to the optimized ligand-receptor match, is to use inhibitors with a higher valency because of the larger functionalized scaffolds in order to target multiple receptor sites simultaneously. A more unspecific mode of binding is required to realize a system that enables an interaction with various types of receptors. One way would be to attach of polycationic architectures to the scaffold in order to achieve an overall positive charge for electrostatic interactions like many viruses.[90] Polycations are well known to easily adhere to the negatively charged cell surface and deliver diagnostic as well as therapeutic agents, or nanoparticles.[91, 92] Furthermore, they are able to form stable polyplexes with siRNA or DNA for transfectional therapy, mainly due to the presence of positive-charge amine functionalities.[91] Unfortunately, application of these polyamines is often restricted because they are more toxic than polyanions, which can result in lysis of the cell membrane.[93, 94]

The other way would be to develop polyanionic architectures with an overall negative charge that is equal to that of the cellular membrane as well as glycocalyx. This leads, on the one hand, to weaker cellular interactions due to repulsion and, on the other, to competitive binding of virus particles. Over the years, it turned out that only envelope viruses like vesicular stomatitis virus (VSV),[95] human immunodeficiency virus (HIV),[96] vaccinia virus (VACV),[97] as well as herpes simplex virus (HSV)[98, 99] are able to interact with polyanions. The reason for this can be attributed to the protein layer which provides the virus particle with positively charged functionalities and simultaneously masks the negatively charged lipid bilayer.[96] So far it looks like the protein interaction differs from virus to virus but, for the most case the mechanism behind this behavior is still unclear.

In the case of HIV-1, the variable loop V3 of the surface glycoprotein gp120 was identified to be responsible for the membrane fusion and virus entry into human lymphocytes or macrophages.[100] In this connection Moulard[101] et al. demonstrated that gp120 is able to bind polyanions selectively, which was confirmed by Lüscher-Mattli[96] due to inhibition experiments of various polyanionic architectures such as negatively charged proteins, inorganic polyphosphates, or sulfated polysaccharides and polymers.

Whereby the polysulfated system reached the highest inhibition potential, while phosphonates only showed a weak or no inhibition for different types of enveloped viruses.[96, 102] The reason for the good inhibition potential of polysulfates can most likely be attributed to the affinity of envelope viruses to bind relatively unspecific to heparan sulfate on the surface of the extracellular matrix.[99, 103]

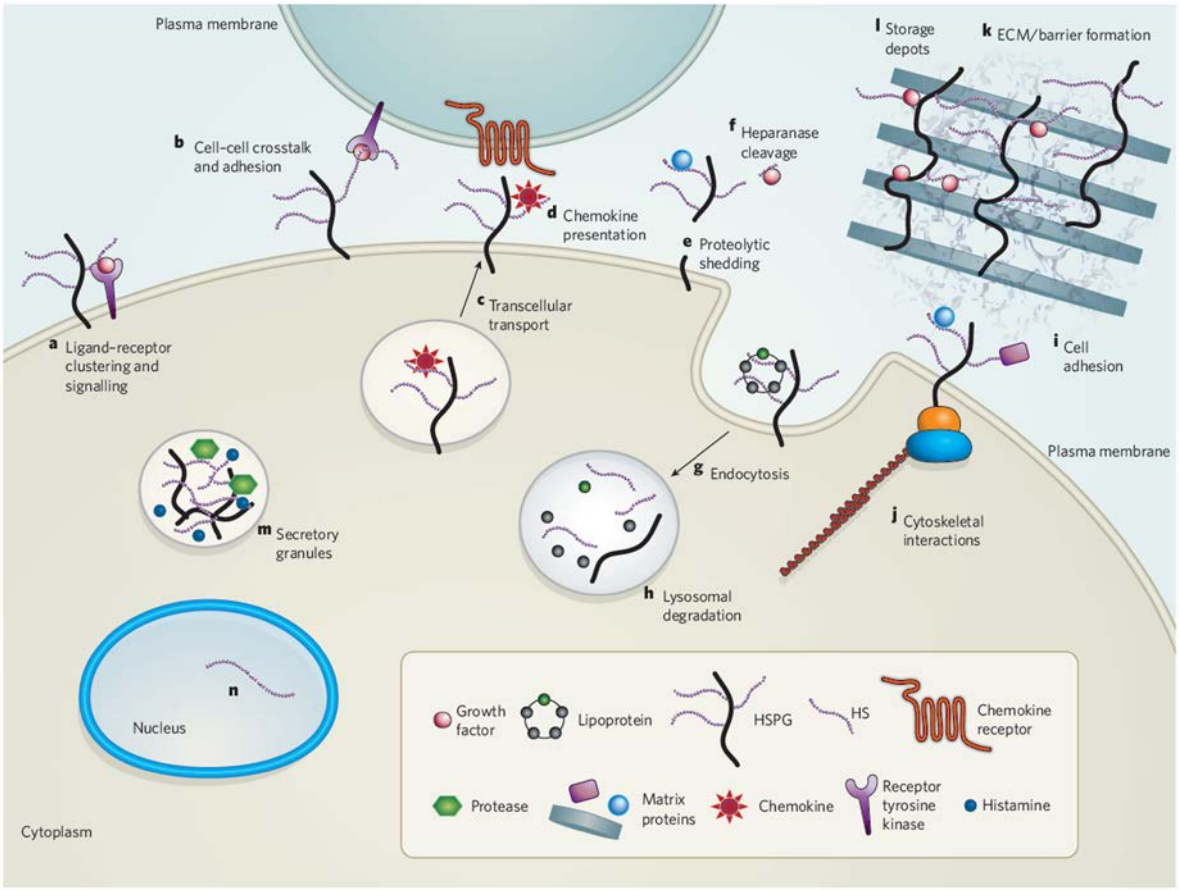

Figure 6. Functions of heparan sulfate proteoglycans in mammalian cells: (a) HSPGs can act as a coreceptor for growth factors and (b) enable cell-cell crosstalk with neighboring cells. (c) They transport chemokines across cells and (d) place them on the cell surface. (e) Syndecans and glypicans can be shedded from the cell surface and (f) where the HS is cleaved by heparanase and bound ligands are released. (g) The shedded glycans can be taken up by endocytosis and (h) then degraded in the lysosomes. (i) HS chains are also involved in the cell adhesion to the ECM and (j) are able form bridges to the cytoskeleton. (k) Secreted HSPGs are forming physiological barriers and (l) sequester growth factors and morphogens for later release. (m) Highly sulfated heparin chains are stored in the secretory granules for secretion into the extracellular space. (n) So far it is only speculated that HS chains are even presented in the nucleus for an unknown assignment. Reproduced with permission from Ref. 103, Copyright 2007, Nature Publishing Group.

Heparan sulfate proteoglycans (HSPGs) are a major component of the extracellular matrix (ECM) and play an essential role in various processes.[103] In general, HSPGs consist of a core protein and one or more linear heparan sulfate (HS) chains, which are highly

negatively charged and enable electrostatic interactions with different protein-ligands. Additionally the HSPGs can be divided into three active subfamilies the membrane-spanning proteoglycans, the glycophosphatidylinositol-linked proteoglycans, and the secreted extracellular matrix proteoglycans.[103] Each of them is involved in many processes of the mammalian cell physiology like signaling,[104] formation of physiological barriers,[105] adhesion,[106] or transcellular transport,[107] due to their HS chains as demonstrated in Figure 6.

In summary, the efficacy of a pathogen inhibitor can be varied by different factors such as size, flexibility, ligand distribution, or ligand conformation. Studies by Haag and coworkers recently showed that the geometry of the inhibitor as well as the size ratio of the pathogen compared to the inhibitor system also affect the overall inhibition potential.[73] The development of unspecific binding inhibitors seems to be more applicable than an optimized ligand-receptor-match due to the lack of topological information. Electrostatic interactions could thereby play an essential role, as impressively demonstrated by nature on the example of the highly negatively charged heparan sulfate.

In this work, the focus lies on the development of novel n-valent architectures (n>> 100), which mimic the extracellular matrix and therefore are able to interact with different heparan sulfate-dependent viruses such as vaccinia or herpes viruses. In this connection, different nanomaterials, which are functionalized with dendritic polyglycerol sulfate (dPGS) or its linear analog (lPGS), are evaluated for their inhibitiory efficacy.

1.2.3 Polyglycerol sulfate

As discussed in Chapter 1.2.2, polyanions, especially polysulfates, could be used to develop effective polyvalent inhibitors based on electrostatic interactions. An excellent example for such an efficient polysulfated system is the natural occurring heparin. Heparin is a linear highly sulfated polyglycan showing the highest negative overall charge density of all natural macromolecules.[108] It has been frequently used as viral entry inhibitor as well as a therapeutic for thrombosis over the last decades.[109-113] However, the application of heparin is limited due to several reasons. The most serious disadvantages of heparin are that it has to be isolated from mammalian organs, which always bear the potential risk of a contamination by proteinaceous infectious particles (prions) and the even more important drawback is the strong anti-coagulant effect.[9, 114]

To avoid the anti-coagulant effect and potential contamination by prions, Haag et al. developed a fully synthetic heparin mimetic, that is comparably activity as heparin but lacks heparin's typical side effects.[7] The basic module of the mimetic is represented by polyglycerol (PG), a highly biocompatible and multivalent macromolecule, which can be synthesized in various sizes up to 20 nm (Figure 7).[8] Even sizes in the micrometer range can be realized due to the formation of microgels via crosslinking processes. The excellent water solubility, low toxicity, and multiple free hydroxyl groups, which can be functionalized further by different techniques, make PG a quite variable and suitable architecture for biomedical applications such as drug delivery.[8, 115]

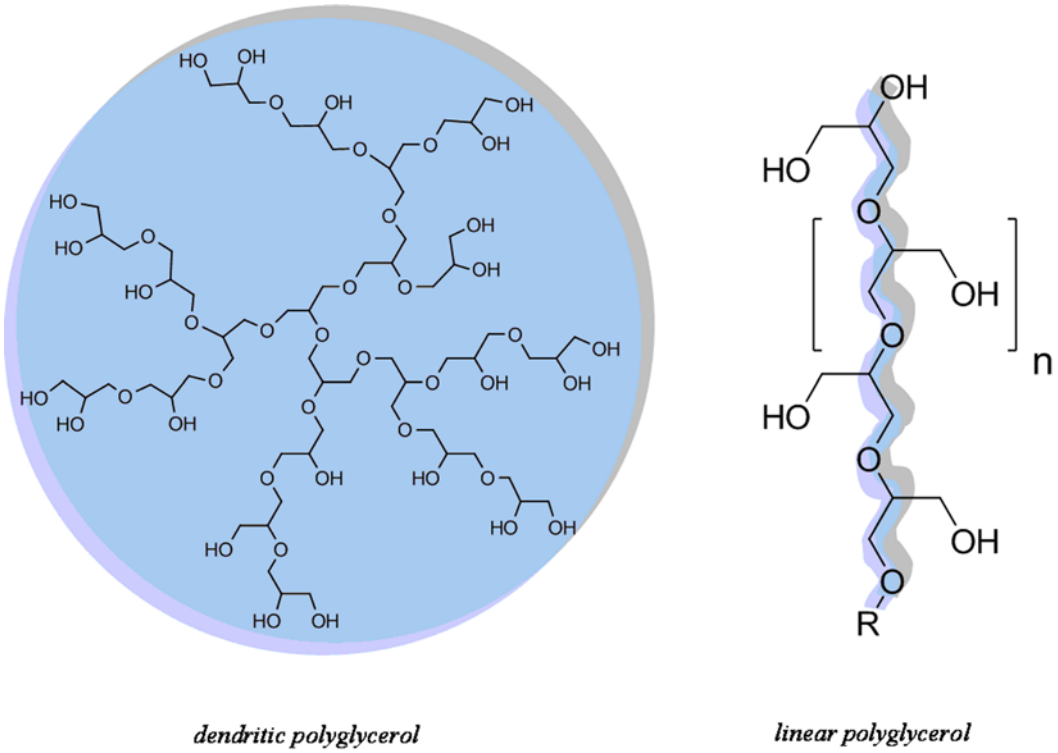

Figure 7. Schematic representation of the molecular structure of dendritic and linear polyglycerol.

The desired synthetic heparin analog can be achieved by a simple polysulfation of dendritic PG that was established by Alban et al.[7] using a SO_3/pyridine complex under dry conditions. During this process, a targeted amount of the suitable hydroxl groups was converted into sulfates, which led to an highly overall negative surface charge. The sulfated dPG still showed a very low cytotoxicity, even at degrees of sulfation (DoS) higher than 90%.[116] Additionally, it did not affect the cellular morphology as well as the cell number, and exhibited a high binding affinity to L- and P-selectin on a low nanomolar level due to its sulfate functionalities.[114, 116] The present sulfate groups on the dPGS periphery (Figure 8) were also able to interact with several proteins in the complementary system,

leukocytes, and VSV viruses via electrostatic interactions.[8, 114] As discussed in Chapter 1.2.2 polysulfates have high potential to be considered for novel pathogen inhibitors. However, the small size and the spherical shape of dPGS could be limiting factors for the inhibition efficacy, since the largest particles, that have been synthesized so far are below 20 nm in size and therefore much smaller than most viruses.

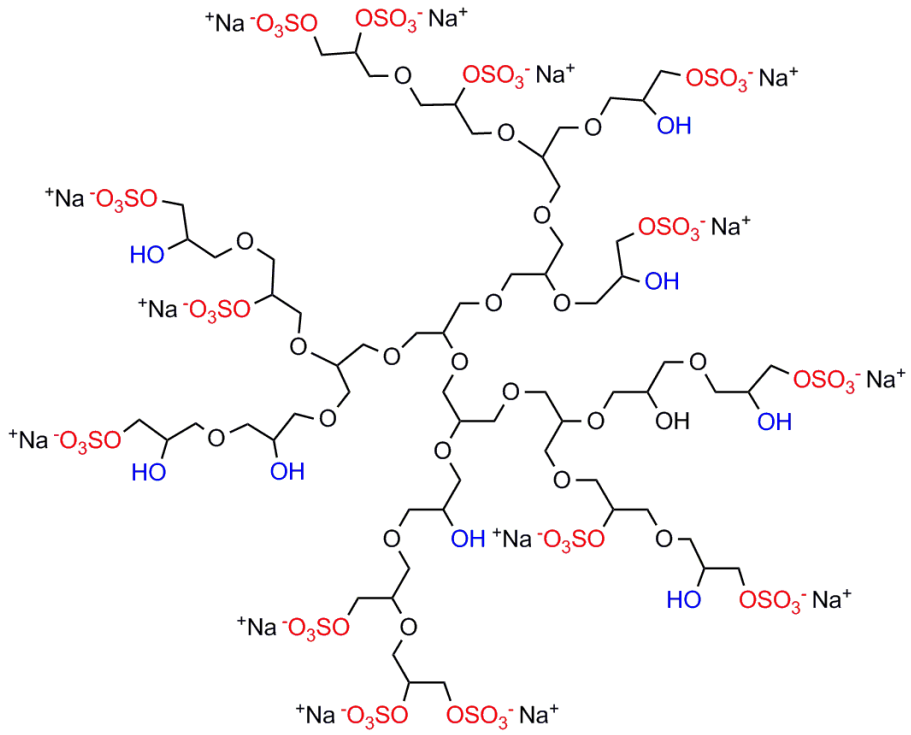

Figure 8. Schematic molecular structure of dendritic polyglycerol sulfate, exhibiting hydroxyl groups (blue) and sulfates (red) on its periphery.

The right geometry, a large contact area between the targeted pathogen and the inhibitor, and an optimized pathogen-inhibitor-size ratio are essential elements for developing an efficient inhibitor system (see Figure 5).[89] For this reason, flexible polysulfated systems that operate in pathogen- or cell-like dimensions need to be developed and will be discussed later in this thesis. Therefore the focus lies on combining different carbon nanomaterials with the biologically active properties of sulfated polyglycerols.

1.3 Polyvalent carbon-based virus inhibitors

1.3.1 Design of polymeric 0D, 1D and 2D architectures

The previous sections already pointed out that multivalent interactions are frequently used by nature for various biological processes. One of the most important is the adhesion process of viruses[75, 76] and bacteria[77, 78] to a targeted cell. To avoid this adhesion, novel inhibitors are required that are able to bind the pathogen and therefore inhibit its cell entry. As already discussed in this work, there are several parameters, which can significantly affect the inhibition efficacy and are therefore essential for new inhibitor designs. In this connection one of the biggest challenges is the enlargement of the inhibitor size to virus- or cell-like dimensions. Studies by Haag et al.[73] recently showed the dependency of the inhibitor geometry as well as the pathogen-inhibitor size ratio.

To face this problem new extracellular matrix inspired inhibitors have been developed by combining different nanomaterials with polyglycerol sulfates.

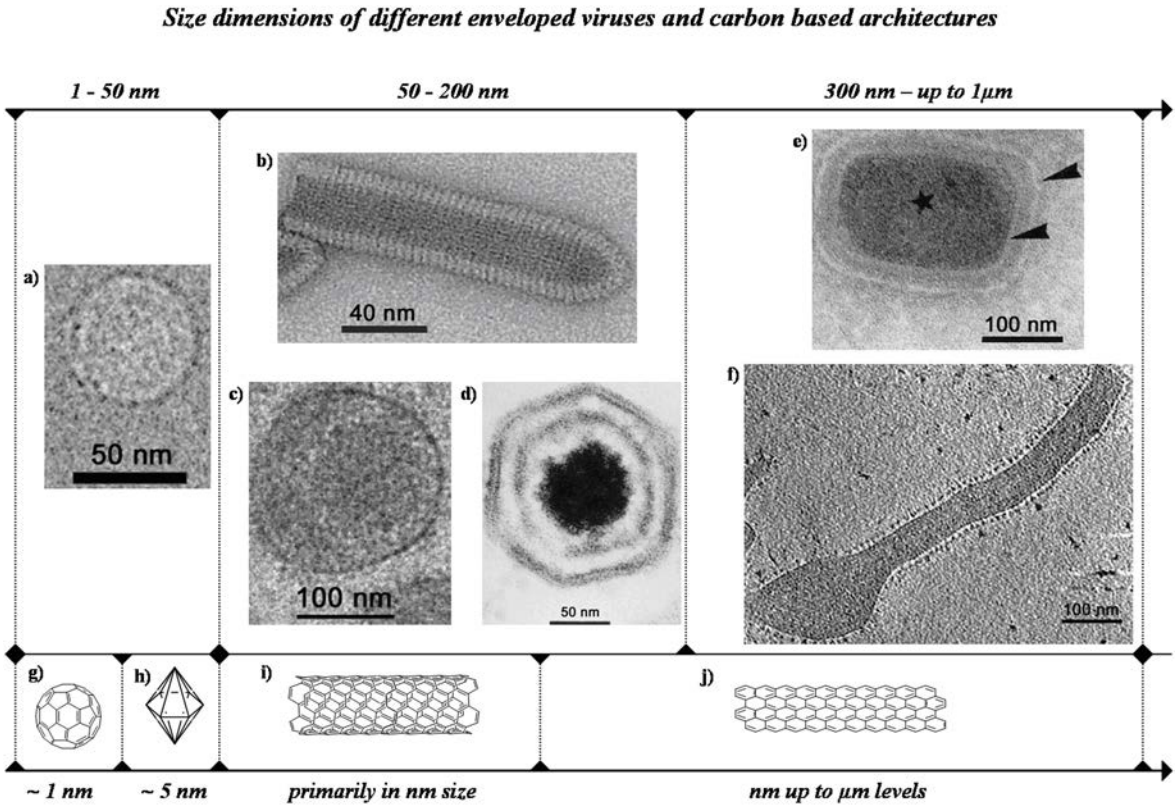

Figure 9. CryoEM micorgraphs of different sized enveloped viruses (a - f) and schematic representation of different sized carbon based architectures (g – j): (a) Zika virus (ZIKV), (b) vesicular stomatis virus (VSV), (c) herpes simplex virus type 1 (HSV-1), (d) African swine fever virus (ASFV), (e) vaccinia virus (VACV), (f) Ebola virus (EBOV), (g) C_{60} Buckyball, (h) detonation nanodiamond, (i) carbon nanotube, and (j) graphene sheet. Reproduced with permission from: a) Ref. 117, © 2016, and b) Ref. 118, © 2013, Nature

Publishing Group; c) Ref. 119, © 2003, The American Association for the Advancement of Science; d) Ref. 120 © 1998, e) Ref. 121 © 2001, and f) Ref. 122 © 2014, American Society for Microbiology.

Due to the combination of the nanomaterial's unique properties[34, 42-44, 62] and biological active properties of the polyglycerol sulfates,[7, 114] different inhibitor designs become feasible.

In this context, the fullerenes as well as the detonation nanodiamonds represent zero-dimensional, spherical scaffolds ranging in 1 nm and 4 - 6 nm in size, respectively, which exhibit unique physical properties and a tuneable surface area up to 420 m^2/g.[34, 60, 68, 69] Furthermore, both nanomaterials are known for their high aggregation tendency which could be advantageous for the inhibitor development because the overall architecture could reach virus- or cell-like dimensions. In general, these globular inhibitor systems should be able to simultaneously bind several receptor sites and additionally decrease the access for further binding due to their rigidity (Figure 5c). Nevertheless, globular inhibitors cannot reach the high contact areas that is possible for the one- or two-dimensional architectures.

The functionalized carbon nanotubes can be described as one-dimensional inhibitor systems that range from nanometer up to centimeter in size and exhibit a high flexibility. Their fluctuating conformations enable access to numerous receptors at the same time and additionally shield further binding sites.

However, a flexible 2D architecture like a functionalized thermally reduced graphene sheet exhibits one additional benefit besides its large contact area, high polyvalent interaction potential, and sterically shielding. The multiple decorated graphene sheet should ideally be able to surround either part of or even the whole infectious particle and thus prevent the pathogen cell adhesion. The high flexibility of the graphene-based hybrid material can be assigned to the functionalization process and can be explained by the partial conversion of the hybridized honeycomb-like lattice from sp^2 to sp^3.[123] Even if it seems like a minor operation, this enables bending, extensively folding, or even wrapping of smaller particles. It can also be assumed that several sheets adhere on one pathogen to fully surround it, if the size of 2D hybrid material is smaller than the infectious particle.

Two procedures can be used to realize all the enumerated polymeric hybrid architectures, namely, on the one hand, the "grafting from" and, on the other, the "grafting to" approach. Both concepts will be discussed in more detail in the next chapter.

1.3.2 Ring-opening multibranching polymerization — "graft from"

The first concept can be described as a “grafting from” approach due to a surface-initiated ring-opening multibranching polymerization (ROMP) as introduced by Huck et al.[124] In this context the polymer architecture is directly built up on the particular scaffold material (see Figure 10). Komatsu and coworkers demonstrated in 2011 on the example of nanodiamonds that this concept is also applicable for nanomaterials.[125] However, the pristine graphite, carbon nanotubes, nanodiamonds, and fullerenes are not suitable for this approach, which is why they have to pretreated by different methods. In the case of graphite, an oxidiation could initially be carried out by using the Hummer's method[25] followed by a thermal reduction[31, 32] to obtain a higher exfoliation and a more uniform surface with multiple hydroxyl groups. Similar harsh conditions are also suitable for carbon nanotubes[57, 126] and nanodiamonds[125, 127] by using most likely high concentrated mixtures of HNO_3 and H_2SO_4. After the pretreatment of these nanomaterials the polyglycerol grafting can be realized by a thermally driven ROMB polymerization. In contrast, fullerenes can also be functionalized with polyglycerol by using an anionic ring-opening multibranching polymerization as demostrated by Adeli et. al.[41]

The difference between both methods can be located in the initiation step and the deployment of the latent AB_2 structured monomer, namely, glycidol. In the anionic ROMB polymerization potassium *tert*-butoxide (KO*t*Bu) is generally used as initiator and the glycidol has to be added slowly in small droplets.[128] In the thermally driven ROMB polymerization only the monomer in bulk and a weak nucleophile like a suitable hydroxyl group of the pretreated nanomaterials is required. At a temperature of 120 °C, the hydroxyl group of the nanomaterial is able to perform a nucleophilic attack on the β- or γ-carbon of glycidol, which is presented in Figure 10. During this attack the epoxide is opened and two potential products were formed. In this context, it can be assumed that the carbon located in the γ-position to the hydroxyl group of the glycidol is more favored, since it was less substituted and possessed a lower sterical hindrance.[129] Nevertheless a nucleophilic attack on the β-carbon could not be fully excluded. The termination of the polymerization processes is achieved either by quenching or cooling down, which should lead to highly polymer-grafted hybrid nanoarchitectures.

To enable potential electrostatic interactions of these hybrid nanomaterials a simple polysulfation can be performed by using a SO_3/Pyridine complex as described by Alban and coworkers.[7] During this process, a targeted amount of the present hydroxyl groups in

the polymeric backbone are converted into sulfates, which lead to a highly overall negative surface charge.

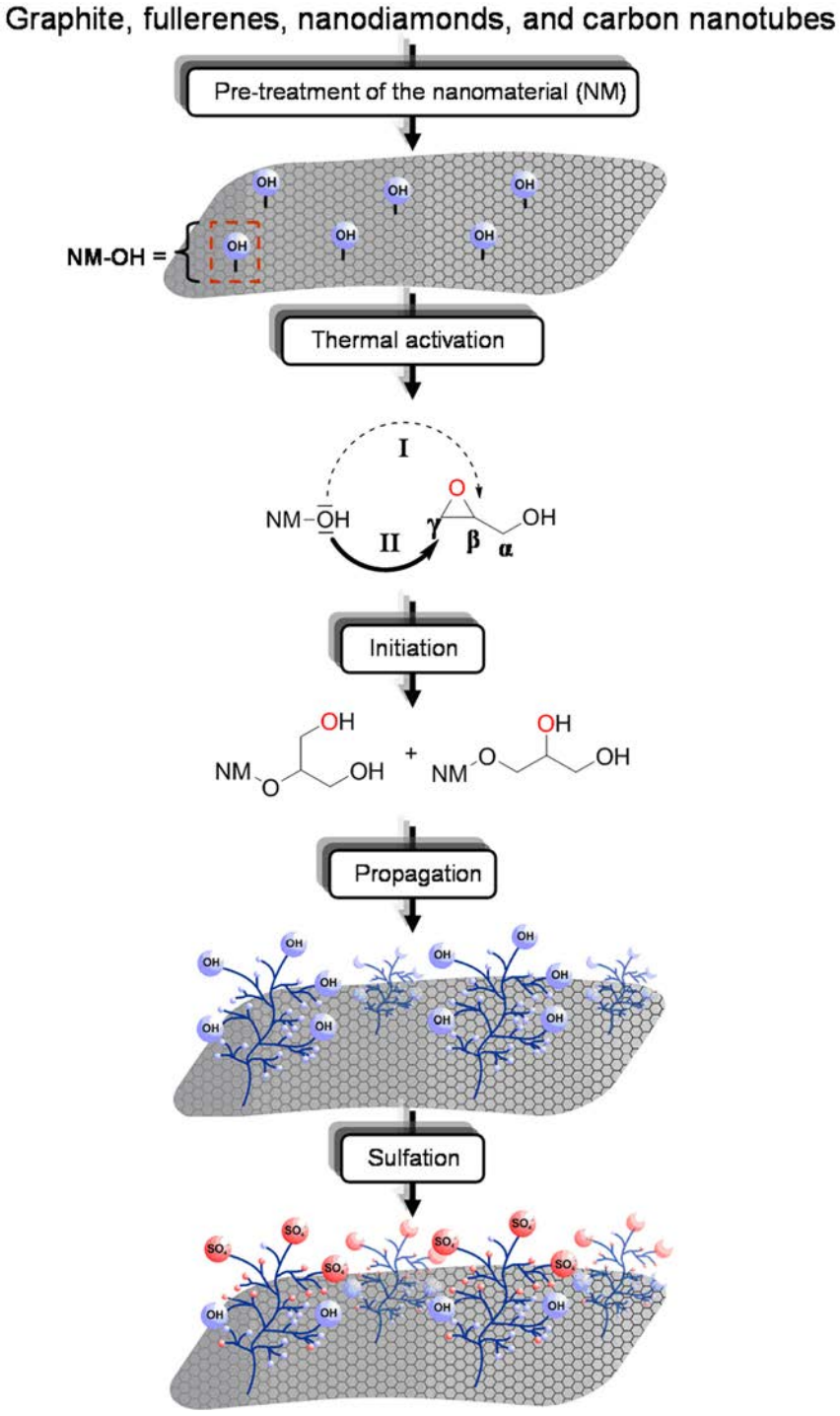

Figure 10. Schematic representation of the intended inhibitor development process, starting from the pristine nanomaterials (graphite, fullerene, nanodiamond, and nanotube) to the polyvalent hybrid architectures. The nanomaterials have to be pretreated by oxidation and/or reduction before a thermally driven ring opening multibranching polymerization can be carried out followed by a sulfation, as presented here on the example of thermally reduced graphene oxide (TRGO).

1.3.3 [2+1] Cycloaddition — "graft to"

An alternative procedure for functionalizing carbon-based nanomaterials is the so-called “grafting to” approach. In contrast to the “grafting from” approach, the desired ligand is directly attached to the nanomaterial and has not to built up on the surface. In general, there are two feasible ways to realize this concept. The first option is a direct post-modification of already existing functionalities on the carbon surface. Thereby, the present epoxy groups, for example, are suitable for covalent modification via a ring-opening reaction in presence of a primary amine derivative.[130] Additionally, amines could also perform an amide formation by reacting with an available carboxly group on the nanomaterial surface. Further procedures like click-chemistry,[131] host-guest complexes,[132] covalent attachments by using either phenyl diazonium derivatives,[133] or diazonium salts followed by an atom transfer radical polymerization are also applicable.[134] Due to fullerene[135] and nanotube[136] research, it is also well known that the conjugated π-system of the nanomaterial can directly be targeted by using a nitrene addition. In the case of graphite oxide even more reactions[137, 138] become possible such as a Diels-Alder reaction on the edges of the sheet-like material.[139, 140]

However, in this work the focus is on the nitrene addition[141-143] and therfore represented in more detail on the example of a thermally reduced graphene sheet, as shown in Figure 11. Due to thermally activation at 160 °C, the azido moities of the polyglycerol azide should be converted into highly reactive nitrenes under the release of nitrogen gas. The high reactivity of the nitrene spezies will initiate a pericyclic [2+1] cycloaddition on one of the carbon double bonds of the nanomaterial. Due to this, an aziridine ring will be formed, which might affect the overall conjugated π-system. It can be assumed that the disordered electron systems will undergo a rearrangement to restore the order of the electronic conjugation of the carbon surface. In the end an analog polysulfation as for the “grafting from” procedure has to be performed to enable the potential pathogen interaction of the functionalized nanoarchitectures.

In summary, two advantages can be exspected for the nitrene addition compared to the described "grafting from" approach. First of all, by using the “grafting to” approach it should be possible to facilitate a defined covalent linkage of an azido-ligand onto the nanomaterial, which generally allows to evaluate the impact of different ligand conformations on the inhibition efficacy. Secondly, the implementation of the FTIR-traceable azido moiety should offer a simple possibility to monitor the reaction conversion.

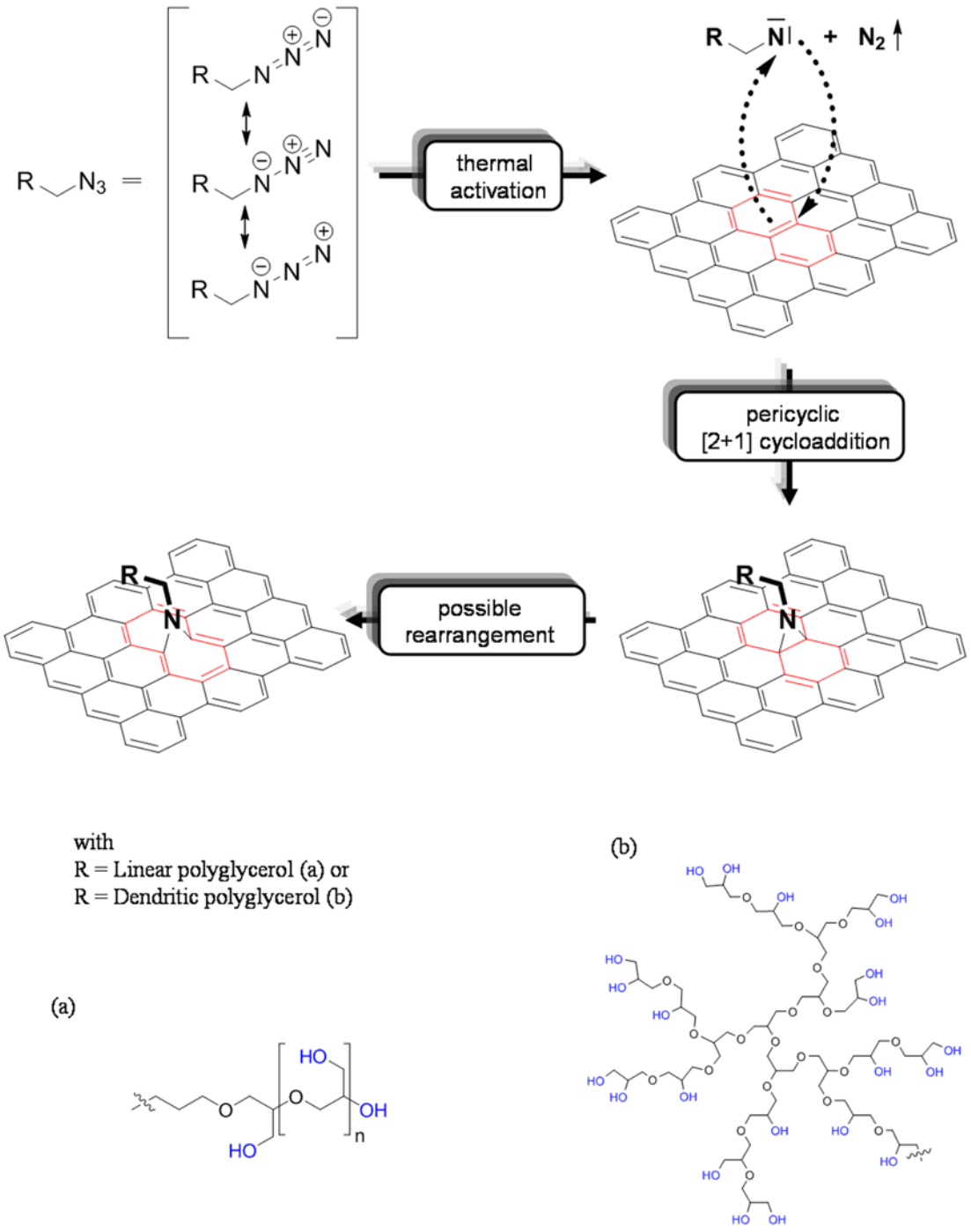

Figure 11. Schematic representation of a proposed mechanism for the functionalization of a graphitic surface by using a nitrene addition. Due to a thermal activation, the azido derivative is transformed into the highly reactive nitrene species resulting in a cheletropic attack on the conjugated π-system of the nanomaterial. An aziridine ring is formed in the process, which has an effect on the overall conjugated π-system. A rearrangement can be assumed to restore the order of the electronic conjugation. (a) and (b) are schematic representations of the molecular structure of linear polyglycerol and dendritic polyglycerol.

1.4 Interaction and inhibition of virus particles

The intended polyvalent architectures should provide an overall negative charge, which is equal to the cellular membrane as well as the glycocalyx, and thereby cause weaker cellular interactions due to repulsion effects. Furthermore, the highly sulfated, grafted polymer backbone of these hybrid nanomaterials should mimic the extracellular matrix and therefore enables potential interaction with different heparan sulfate-dependent viruses. Polyanions are well known to be exclusively capable of interacting with enveloped viruses via electrostatic interactions.[96, 99, 103] In this context, Moulard[101] and Lüscher-Mattli[96] figured out by inhibition experiments of various polyanionic architectures that the polysulfated systems exhibit the highest inhibition potential for different types of enveloped viruses.[102] The reason for this can be attributed, on the one hand, to the protein layer, which provides an overall positive surface charge and simultaneously masks the negatively charged lipid bilayer, and, on the other, to the affinity of the viral proteins to bind relatively unspecifically to heparan sulfate-containing extracellular matrix.[96, 99, 103]

In order to evaluate a potential inhibition efficacy of the intended polyvalent hybrid architectures and to identify the factors, which can have a significant impact on the inhibition potential, binding studies, as well as inhibition experiments with viruses, are essential and have to be performed. In this connection, different types of enveloped viruses should be tested, especially heparan sulfate-oriented viruses should serve as perfect candidates for the biological experiments (e.g. members of the poxviridae and herpesviridae families).

1.4.1 Orthopoxvirus particles

In general, there are four orthopoxviruses that are known to be harmful to humans, namely, vaccinia virus (VACV), monkeypox virus (MPXV), cowpox virus (CPXV), and variola virus (VARV).[144, 145] All of them are members of the poxviridae family and can be classified as enveloped viruses. The whole orthopoxvirus particles have a brick-shaped geometry and a size around 300 - 400 nm in diameter (see Figure 9e).[146, 147] The trimeric viral protein A27 is expressed all over the surface and is known for its high affinity to bind cell-associated heparan sulfate thus enabling the viral uptake into the target cell via endocytosis.[112, 148, 149] Inside the cell, the linear double-stranded DNA genome is released in the cytoplasm where it starts to produce two different types of virions, the intracellular mature virion (IMV) and the extracellular enveloped virion (EEV).[150, 151] Altogether orthopoxvirus particles are interesting candidates for the biological evaluation of the newly

developed inhibitor models due to their high affinity to bind polysulfates by charge interactions of the partially positive charged A27.

1.4.2 Herpesvirus

The family of herpesviridae consists of more than 120 enveloped viruses that are able to infect various species.[152] Eight of them are known to be harmful to humans like the herpes simplex virus type-1 (HSV-1) and -2 (HSV-2),[153] varizella zoster virus (VZV),[154] and cytomegalovirus (CMV).[155] In general, the geometry of a herpesvirus can be described as spherical to pleomorphic with particles ranging from 155 to 240 nm in diameter that contain an icosahedral capsid with a diameter of around 125 nm (see Figure 9c).[119, 156, 157] The virus adheres to the cell by a charge interaction of the viral proteins gB and gC with the extracellular matrix.[158, 159] Both viral proteins provide several positive-charged amino acids that have a high affinity to interact with the present negatively charged heparan sulfate. The virus particle is subsequently taken up via endocytosis, which is followed by the release of linear double-stranded DNA genome into the cytoplasm. [160-164] After the first infection, all herpesviruses establish lifelong latency and cannot be removed from the host via immune elimination, which results in a perseverative disease under stress conditions.[160, 165]. For this reason and due to the lack of anti-viral drugs that can inhibit the herpesvirus entry, a prophylactic entry inhibitor is strongly required.

1.4.3 African swine fever virus

The African swine fever virus (ASFV) is so far the only known member of the asfarviridae family and is one of the enveloped viruses.[166] The general morphology of the ASFV particle is quite similar to the herpesviridae. It is spherical to pleomorphic in shape with a size of 175 to 215 nm in diameter containing an icosahedral capsid with side-to-side dimensions of 172-191 nm (see Figure 9d).[167, 168] For a number of years it was assumed that the viral particles entered the host cells via receptor-mediated endocytosis. New studies by Sánchez et al., however, have proposed a macropinocytic mechanism of endocytosis.[169] Although the exact mechanism for cell entry is not yet known, one can assume that the virus releases the double-stranded DNA genome into the cytoplasm where the replication process is started. As there is no prophylaxis or treatment for ASFV, new inhibitor systems definitely have to be developed.[170]

2. Motivation and Objective

The demand for novel pathogen inhibitors is an urgent and most likely never-ending process in medical science, especially when the usual small monovalent antiviral agents have not shown the desired efficacy. Multivalency could be an optimal solution to improve the efficacy, because most viruses and bacteria exhibit multiple polyvalent binding sites. As described in the introduction, polysulfates could play a major role, like the dendritic polyglycerol sulfate (dPGS),[7] which is already known to be an excellent candidate for targeting inflamed endothelium and may has also the potential to act as virus entry inhibitor for various types of viruses. Nevertheless, it should be mentioned that polysulfates are exclusively capable of interacting with enveloped viruses via charge interaction to positively charged virus binding sites.[96, 99, 103]

However, dPGS can only be synthesized in size dimensions of around 2 - 20 nm so far,[8] and therfore are much smaller than the typical pathogens, which range from 100 nm up to micrometers in size. Due to the studies of Whitesides[4] and Haag,[73] it seems logical that an enlarged polyglycerol sulfate architecture, operating in pathogen- or cell-like dimensions, could act as efficient entry inhibitors. Materials that offer a large surface area and are capable of being functionalized with polyglycerol sulfate are very in demand to enhance the overall contact area and thereby the interaction potential. In this context carbon-based nanomaterials (graphene, nanotubes, nanodiamonds, and fullerenes) could serve as excellent scaffolds possessing high surface areas in different sizes and geometries. In this thesis, the focus is on the development and evaluation of such polyvalent hybrid materials and their antiviral efficacy *in vitro,* especially in the case of the flexible 2D-hybrid architectures. Due to a “grafting from” or “grafting to” approach it should be possible to attach multibranched or linear polyglycerol sulfates on the pre-treated nanomaterial and thereby transfer properties of the biologically active PGS to the combined hybrid-architecture leading to novel, polyvalent pathogen inhibitors. Binding studies as well as inhibition experiments with different viruses could be carried out to evaluate the inhibition efficacy of the individual hybrid materials. Heparan sulfate-dependent viruses like orthopox or herpes virus should be ideal candidates for these biological studies, since the general inhibitor design was intended as heparin mimetic to imitate the heparan sulfate-containing extracellular matrix. These novel architectures could ultimatively lead to the wrapping of the virus (see Figure 12)

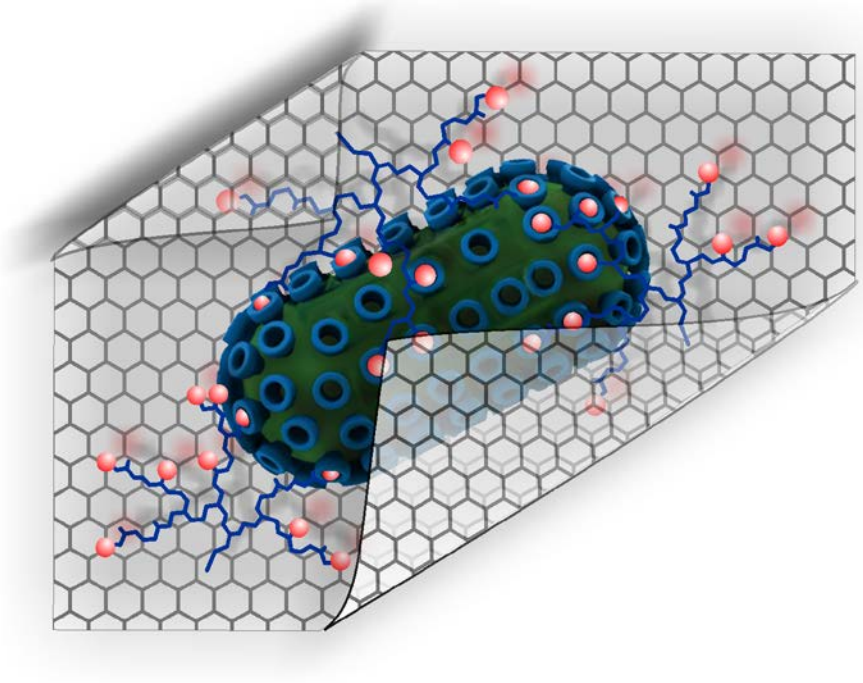

Figure 12. Schematic representation of a polysulfated graphene-based hybrid architecture that mimics the heparan sulfate-containing cell surface and thereby serves as an efficient polyvalent 2D inhibitors for various types of heparan sulfate binding viruses like the illustrated orthopoxvirus.

The three main objectives of this thesis were (a) to develop novel polyvalent 2D inhibitors that mimic the extracellular matrix to inhibit heparan sulfate-dependent viruses by combining carbon nanomaterials with polyglycerol sulfates. (b) Modification of the inhibitor design by varying the degree of sulfation and polymerization, inhibitor sizes, and ligand conformation by using polysulfate functionalized graphene sheets as model systems to identify which parameters can directly and significantly affect the inhibition efficacy. (c) Synthesis and evaluation of further potent pathogen inhibitors in the form of PGS-coated nanomaterials differing in size and geometry like nanodiamonds, fullerenes, and nanotubes.

3. Publications

In this chapter all published articles and submitted manuscripts are listed.

3.1 Highly Efficient Multivalent 2D Nanosystems for Inhibition of Orthopoxvirus Particles

Benjamin Ziem,[#] Hendrik Thien,[#] Katharina Achazi, Constanze Yue, Daniel Stern, Kim Silberreis, Mohammad Fardin Gholami, Fabian Beckert, Dominic Gröger, Rolf Mülhaupt, Jürgen P. Rabe, Andreas Nitsche, and Rainer Haag, *Adv. Healthcare Mater*. **2016**, 5,2922-2930. [#] These authors contributed equally.

http://dx.doi.org/10.1002/adhm.201600812

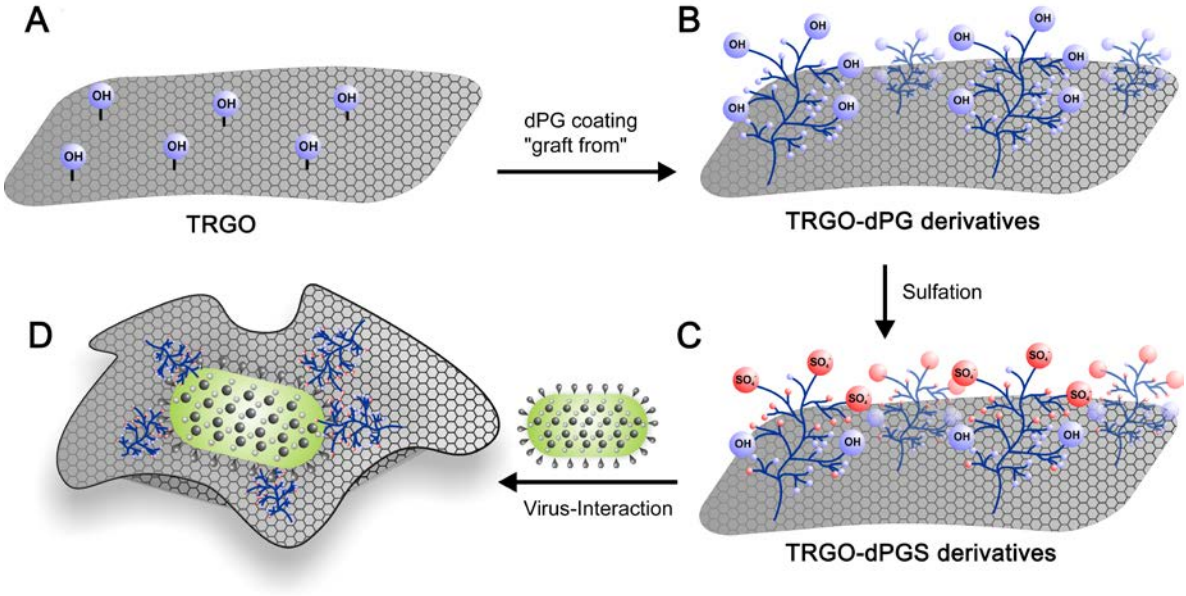

Figure 13. Schematic representation of the inhibitor development process: (A) Thermally reduced graphene oxide (TRGO) was functionalized with polyglycerol by using a simple "grafting from" approach to form (B) TRGO-dPG. Due to a polysulfation TRGO-dPG was converted to TRGO-dPGS which is able to (D) interact with orthopoxvirus particle. Reproduced with permission from Ref. 171, Copyright 2016, John Wiley and Sons.

In this publication the author contributed with:

- The research design,
- synthesis of all 2D nanosystems,
- synthesis of biotinylated dPG,
- characterization of all compounds,
- coordination of the cooperations,
- discussion and evaluation of the results,
- preparation of the manuscript.

3.2 Size-dependent Inhibition of Herpesvirus Cellular Entry by Polyvalent Nanoarchitectures

Benjamin Ziem, Walid Azab, Mohammad F. Gholami, Jürgen P. Rabe, Klaus Osterrieder, and Rainer Haag, *Nanoscale*, **2017**, 9, 3774-3783.
http://dx.doi.org/10.1039/C7NR00611J

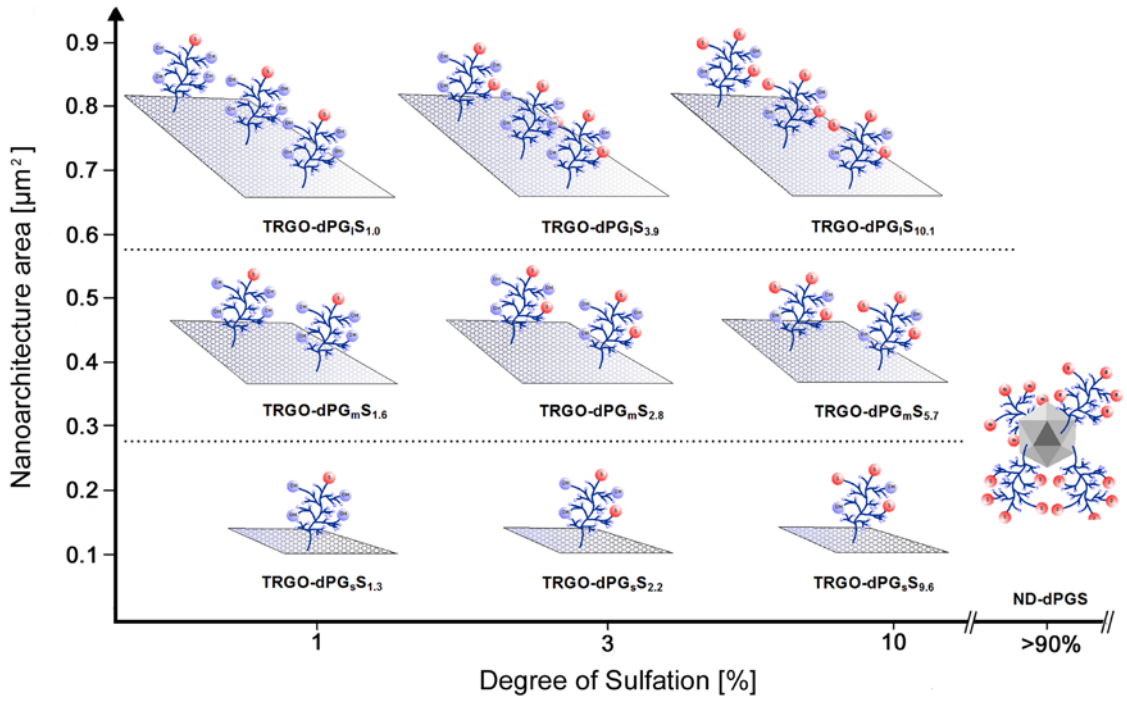

Figure 14. Schematic overview of synthesized polyvalent hybrid nanoarchitectures varying in their size and degree of sulfation.

In this publication the author contributed with:

- The research design,
- synthesis of all nanoarchitectures,
- characterization of all compounds,
- coordination of the cooperations,
- discussion and evaluation of the results,
- preparation of the manuscript.

3.3 Polyvalent 2D Architectures for Inhibition of Pseudorabies and African Swine Fever Virus

Benjamin Ziem, Jessica Rahn, Ievgen Donskyi, Kim Silberreis, Luis Cuellar, Jens Dernedde, Thomas C. Mettenleiter, and Rainer Haag, *Macromol. Biosci.*, **2017**. http://dx.doi.org/10.1002/mabi.201600499

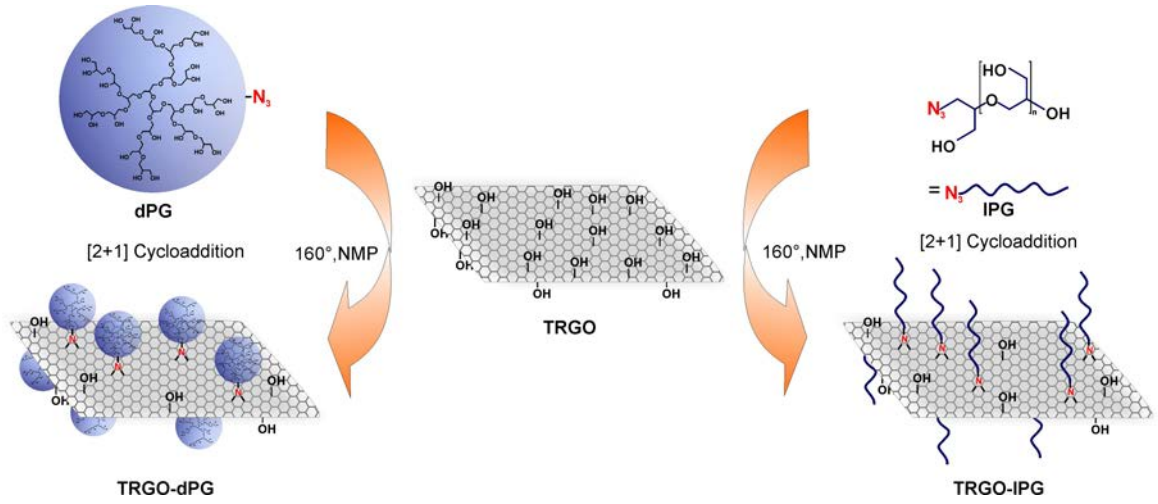

Figure 15. Schematic representation of the inhibitor development by combining thermally reduced graphene oxide (TRGO) with either dendritic polyglycerol (dPG) azide or linear polyglycerol (lPG) azide.

In this publication the author contributed with:

- The research design,
- synthesis of all nanoarchitectures,
- characterization of all compounds,
- coordination of the cooperations,
- discussion and evaluation of the results,
- preparation of the manuscript.

4. Summary and Perspective

The development of new efficient inhibitor systems for pathogens is a complex task. As shown in this work, there are many parameters that can significantly affect the inhibition efficacy and must therefore be considered during the development process for novel inhibitor designs.

The main objective of this work was the development of new polyvalent nanoarchitectures by combining different nanomaterials with the bioactive dendritic polyglycerol to generate potent virus entry inhibitors. These inhibitors mimic the extracellular matrix and therefore are able to inhibit heparan sulfate-dependent viruses. The evaluation of the individual inhibition efficacies was carried out by various biological experiments. Additionally, the graphene-based inhibitor architectures served as model systems which was systematically varied to evaluate the impact on the inhibitiory efficacy due to changes in the degrees of sulfation and polymerization, inhibitor sizes, and ligand structure. The complete synthesis and evaluation process of this thesis can be described by the following four projects:

The first project immediately showed the demand for novel hybrid architectures, because free polyglycerol sulfate was only able to bind to the viral protein A27 of orthopoxviruses but did not show any inhibition effect in the plaque reduction and neutralization tests (PRNT). However, after grafting the polyglycerol sulfate on the thermally reduced graphene sheet, the novel 2D polymer architecture demonstrated a strong inhibition of orthopoxvirus particles. In order to exclude effects from the graphene material, the same biological experiments and investigations were carried out also for the unsulfated analog architecture. According to this, the sulfate moieties were responsible for the strong interactions with viral membrane protein A27 of the different tested orthopoxviruses (VACV, CPXV, and MPXV). Furthermore, it could be demonstrated in this project that both the degree of sulfation and the degree of polymerization have a strong influence on the binding efficiency. By increasing these parameters, a higher binding could be achieved as was shown in a competive binding assay.

One of the biggest challenges in the general development process of a new inhibitor system is the adaption of the inhibitor size to virus- or cell-like dimensions. For this reason, the second project dealt with size-dependent inhibition of herpes viruses by polyvalent nanoarchitectures. By a simple "grafting from" approach, TRGO as well as nanodiamonds were functionalized with polyglycerol first and subsequently converted into their sulfated analogs. Both inhibitors designs mimicked the extracellular matrix and thereby were able to

interact with the viral proteins gB and gC, which are known for their high binding affinities to the heparan sulfate-containing extracellular matrix. Due to this, an efficient binding as well as a strong inhibition for herpes simplex virus type-1 (HSV-1) and equine herpes virus type-1 (EHV-1) could be observed in the biological studies. For evaluating a potential size effect on the inhibition efficacy, three graphene-based inhibitors of different sizes were investigated. It could be clearly demonstrated that the smaller inhibitor systems exhibited a higher inhibition, which could be explained, on the one hand, by the inhibitor-virus-size ratio and, on the other, by a possible correlation to the required energy for bending the functionalized TRGO sheets. Based on the physical evaluation, it could be assumed that the smaller functionalized graphene derivatives had a higher ratio of interacting areas compared to non interacting areas and thereby were more energy efficient, which resulted in a higher virus inhibition.

In the third project, graphene sheets were functionalized, on the one hand, with dendritic polyglycerol sulfate and, on the other, with linear polyglycerol sulfate by using a "grafting to" approach in the form of a nitrene addition. Thereby polyglycerol azide was directly attached to the conjugated π-system of the nanomaterial via a pericyclic [2+1] cycloaddition. To evaluate the effect of the ligand conformation on the overall inhibition potential, equal molecular masses as well as the same degree of sulfation were used for the attached polyglycerol sulfate derivatives. Both derivatives were tested in plaque reduction assays for two different types of viruses. In the case of the African swine fever virus (ASFV), the two potential entry inhibitors showed the same inhibition behavior. But in the case of the pseudorabies virus (PrV), both functionalized derivatives reached a strong inhibition (> 90%). The dendritic architecture, however, required a 100 times higher concentration than the linear analog. It can be assumed that the linear conformation of the attached linear polyglycerol sulfate was the reason for the higher efficacy since the viral proteins gB and gC of the PrV are known to bind heparan sulfate which is expressed as linear chains in the extracellular matrix. Furthermore, the blood clotting assay showed that the both derivatives are superior to heparin due to their lower anticoagulant effect.

The fourth project dealt with the synthesis and evaluation of further potent pathogen inhibitors by combining fullerenes as well as nanotubes with polyglycerol sulfates. The functionalized fullerenes can be described as a zero-dimensional architecture that has a high tendency to form aggregates quite similar to the functionalized nanodiamonds. The developed nanotube hybrid material is an one-dimensional inhibitor system, which exhibits high flexibility and pathogen-like dimensions. It can also simultaneously access numerous

receptors and shield further binding sites. Both inhibitor designs were successfully synthesized and are currently under investigations. Based on the results of the first inhibition experiments with HSV-1 and EHV-1 the functionalized fullerenes are not so efficient compared to the nanodiamond analogs. In case of the functionalized nanotubes strong inhibition was obeserved similar to the well investigated graphene-based architectures.

Overall, it could be shown that the novel hybrid architectures have a high potential to bind and inhibit various types of viruses. Additionally, it could be demonstrated that the binding efficiency and the inhibition potential of these systems can be varied at least by the four identified parameters, namely, degree of sulfation, polymer loading, inhibitor size, and ligand conformation. Due to these facts, the concept of developing efficient entry inhibitors based on combining carbon nanomaterials with polyglycerol sulfates was successful.

The results presented in this work already demonstrated that many factors could significantly affect the binding and inhibition efficacy. In this context the novel hybrid architectures represent a well-modifiable inhibitor design, which is already able to interact and inhibit different types of viruses. Nevertheless, the inhibitor design can be further improved by implementing, for example, more specific targeting moieties such as peptides or sugar ligands. Furthermore, zwitterionic polymers attached to the carbon nanomaterials might be used against a wider spectrum of pathogens.

Also, it would be very important to investigate the mechanism for bending, folding, and wrapping of the 2D architectures in more detail. The understanding of the mechanics is the key for developing not only novel inhibitors but also new types of graphene-based nanomaterials.

Additionally, further biological studies and physical experiments should be carried out for the 0D and 1D inhibitor systems and the results should be compared to the 2D inhibitors to evaluate the effect of different geometries. Based on all findings, applications such as filtration, detection or inhibition in healthcare and environmental protection seem to be realistic in the near future .

5. Abstract

In the present dissertation, various carbon nanomaterials (graphene, nanodiamonds, nanotubes, and fullerenes) were initially pre-treated with different oxidative or reductive procedures. The resulting nanostructures were subsequently functionalized by a “grafting from” or “grafting to” process to synthesize novel polymer-hybrid-architectures. By applying a simple polysulfation, it was possible to convert the existing hydroxyl groups of the polymer backbone in an almost precise and controlled manner into sulfate groups. Therefore, the functionalized zero-dimensional nanodiamonds or fullerenes, one-dimensional nanotubes, and two-dimensional graphene hybrid-materials gained an anionic character, which enabled the polyvalent interaction potential of the functionalized nanoarchitectures to different types of pathogens.

By imitating the heparan sulfate-containing extracellular matrix, the synthesized, polyvalent polymer-nanoarchitectures can be seen as an alternative heparin mimetic and thus as a novel pathogen inhibitors. In order to evaluate the inhibition efficacy of the individual hybrid material, binding studies as well as inhibition experiments with different viruses were carried out. Orthopox viruses, herpes viruses, and the African swine fever virus were selected and used for the biological studies, since polyanions only interact with enveloped viruses. Additionally, all of the enumerated viruses have an affinity for heparan-sulfate interaction and are therefore ideal candidates for the efficacy studies of the hybrid-nanomaterials. By varying the novel inhibitory concept and its biological evaluation, it was possible to successfully determine which factors had a significant impact on the inhibition potential. Above all, the degree of sulfation and polymerization as well as the inhibitor geometry and size played a decisive role. Furthermore, in the case of the graphene derivatives, a dependence of the inhibition efficacy due to the attached ligand flexibility could also be shown. Altogether, it can be concluded that by functionalizing the unique carbon nanomaterials with polyglycerol sulfate (PGS) it was possible to transfer properties of the biologically active PGS to the combined system and thus to realize novel, polyvalent pathogen inhibitors. In the near future the collected findings can make a decisive contribution to the development and optimization of efficient, polyvalent inhibitor systems.

6. Kurzfassung

Im Rahmen der vorliegenden Dissertation wurden zunächst verschiedene Kohlenstoff-Nanomaterialien (Graphene, Nanodiamanten, Nanoröhren und Fullerene) mittels unterschiedlicher Oxidations- beziehungsweise Reduktionsverfahren vorbehandelt. Die hierbei erhaltenen Nanostrukturen wurden anschließend einem "grafting from" oder einem "grafting to" Prozess unterzogen, um neuartige Polymer-Hybridarchitekturen zu synthetisieren. Durch Anwendung einer einfachen Polysulfatierung ist es möglich die vorhandenen Hydroxylgruppen des Polymergerüstes zielgerichtet und kontrolliert in Sulfatgruppen umzuwandeln. Die funktionalisierten nulldimensionalen (Nanodiamanten und Fullerene), eindimensionalen (Nanoröhren) und zweidimensionalen (Graphene) Hybridsysteme erhalten dadurch einen anionischen Charakter, der den Hybridmaterialien eine Interaktion mit den überwiegend positiv geladenen Virushüllen ermöglicht.

Durch Imitation der heparansulfathaltigen, extrazellulären Matrix, stellen die synthetisierten, polyvalenten Polymer-Nanoarchitekturen potentielle ECM-Mimetika und somit neuartige Pathogeninhibitoren dar. Um die Wirksamkeit der einzelnen Hybridarchitekturen in Bezug auf ihr mögliches Inhibitionspotential zu testen, wurden sowohl Bindungsstudien als auch Inhibitionsversuche mit unterschiedlichen Viren durchgeführt.

Da Polyanionen ausschließlich in der Lage sind mit eingehüllten Viren zu interagieren, wurden in diesem Zusammenhang sowohl Orthopockenviren, als auch Herpesviren und das Afrikanische Schweinefiebervirus verwendet. Die aufgezählten Virenarten verfügen alle über eine hohe Affinität zu Heparansulfat und sind daher ideale Kandidaten für die Wirksamkeitsuntersuchungen der Hybrid-Nanomaterialien. Durch Variation des neuartigen Inhibitorkonzepts und dessen biologischer Evaluation konnte erfolgreich gezeigt werden, welche Faktoren einen signifikanten Einfluss auf das Inhibitionspotential haben. Hierbei spielen vor allem der Sulfatierungs- und der Polymerisationsgrad als auch die Inhibitorgeometrie und -größe eine entscheidende Rolle. Des Weiteren konnte im Falle der Graphenderivate auch eine Abhängigkeit der Inhibition von der Ligandenstruktur gezeigt werden. Insgesamt lässt sich also festhalten, dass es durch eine Funktionalisierung der einzigartigen Kohlenstoff-Nanomaterialien mit Polyglycerinsulfat (PGS) möglich ist, Eigenschaften des biologisch aktiven PGS auf das Gesamtsystem zu übertragen, um somit neuartige, polyvalente Inhibitoren zu realisieren. Die gesammelten Erkenntnisse können hierbei zukünftig einen entscheidenden Beitrag zur Entwicklung und Optimierung effizienter, polyvalenter Virus-Inhibitoren leisten.

7. References

[1] A. Hafner, J. Lovrić, G. P. Lakoš, I. Pepić, *Int. J. Nanomed.* **2014**, *9*, 1005-1023.

[2] W. Lu, C. M. Lieber, *Nat. Mater.* **2007**, *6*, 841-850.

[3] P. Morganti, *Clin. Cosmet. Investig. Dermatol.* **2010**, *3*, 5-13.

[4] G. Y. Yurkov, A.S. Fionov, Y. A. Koksharov, V. V. Koleso, S. P. Gubin, *Inorg Mater* **2007**, *43*, 834-844.

[5] M. Mammen, S. K. Choi, G. M. Whitesides, *Angew Chem Int Edit.* **1998**, *37*, 2754-2794.

[6] C. Fasting, C. A. Schalley, M. Weber, O. Seitz, S. Hecht, B. Koksch, J. Dernedde, C. Graf, E.-W. Knapp, R. Haag, *Angew. Chem. Int. Ed.* 2012, *51*, 10472-10498.

[7] H. Turk, R. Haag, S. Alban, *Bioconjug. Chem.* **2004**, *15*, 162-167.

[8] M. Calderon, M. A. Quadir, S. K. Sharma, R. Haag, Adv. Mater. **2010**, *22*, 190-218.

[9] R. K. Kainthan, J. Janzen, E. Levin, D. V. Devine, D. E. Brooks, *Biomacromolecules* **2006**, *7*, 703-709.

[10] R. M. Nelson, O. Cecconi, W. G. Roberts, A. Aruffo, R. J. Linhardt, M. P. Bevilacqua, *Blood* **1993**, *82*, 3253-3258.

[11] D. L. Rabenstein, *Nat. Prod. Rep.* **2002**, *19*, 312-331.

[12] S. S. Weinberg, *The Stone Age in the Agean*, 10th ed.; Cambridge University Press: Cambridge, **2007**; *Vol. 1*, 607-608.

[13] K. S. Novoselov, A. K. Geim, S. V. Morozov, D. Jiang, Y. Zhang, S. V. Dubonos, I. V. Grigorieva, A. A. Firsov, *Science* **2004**, *306*, 666-669.

[14] H.-P. Boehm, R. Setton, B. Stumpp, *Pure Appl. Chem.* **1994**, *66*, 1893-1901.

[15] A. K. Geim, K. S. Novoselov, *Nature Mater.* **2007**, *6*, 183-191.

[16] R. D. Dreyer, S. Park, C. W. Bielawski, R. S. Ruoff, *Chem. Rev. Soc.* **2010**, *39*, 228-240.

[17] G. Wang, J. Yang, J. Park, X. Gou, B. Wang, H. Liu, J. Yao, *J. Phys. Chem. C* **2008**, *112*, 8192-8195.

[18] G. Wang, X. Shen, B. Wang, J. Yao, J. Park, *Carbon* **2009**, *47*, 1359-1364.

[19] X. Li, X. Wang, L. Zhang, S. Lee, H. Dai, *Science* **2008**, *319*, 1229-1232.

[20] P. Blake, P. D. Brimicombe, R. R. Nair, T. J. Booth, D. Jiang, F. Schedin, L. A. Ponomarenko, S. V. Morozov, H. F. Gleeson, E. W. Hill, A. K. Geim, K. S. Novoselov, *Nano Lett.* **2008**, *8*, 1704-1708.

[21] D. Li, M. B. Muller, S. Gijle, R. B. Kaner, G. G. Wallace, *Nat. Nanotechnol.* **2008**, *3*, 101-105.

[22] W. Choi, I. Lahiri, R. Seelaboyina, Y. S. Kang, *Crit. Rev .Sol. State. Mater. Sci.* **2010**, *35*, 52-71.

[23] B. C. Brodie, *Ann. Chim. Phys.* **1855**, *45*, 351-353.

[24] L. Staudenmaier, *Ber. Dtsch. Chem. Ges.* **1898**, *31*, 1481-1487.

[25] W. S. Hummers, R. E. Offeman, *J. Am. Chem. Soc.* **1958**, *80*, 1339.

[26] U. Hofmann, Frenzel, A.; Csala´n, *E. Liebigs Ann. Chem.* **1934**, *510*, 1-41.

[27] A. Lerf, H. Y. He, M. Forster, J. Klinowski, *J Phys Chem B* **1998**, *102*, 4477-4482.

[28] H.-P. Boehm,W. Scholz, *Z. Anorg. Allg. Chem.* **1965**, *335*, 74-79.

[29] T. Kuila, S. Bose, A. K. Mishra, P. Khanra, N. H. Kim, J. H. Lee, Prog. Mater. Sci. **2012**, *57*, 1061-1105.

[30] X. Fan, W. Peng, Y. Li, X. Li, S.Wang, G. Zhang, F. Zhang, *Adv. Mater.* **2008**, *20*, 4490-4493.

[31] H.-P. Boehm, A. Clauss, G. O. Fischer, U. Hofmann, *Z. Anorg. Allg. Chem.* **1962**, *316*, 119-127.

[28] H.-P. Boehm,W. Scholz, *Z. Anorg. Allg. Chem.* **1965**, *335*, 74-79.

[32] M. J. McAllister, J.-L. Li, D. H. Adamson, H. C. Schniepp, A. A. Abdala, J. Liu, M. Herrera-Alonso, D. L. Milius, R. Car, R. K. Prud'homme, I. A. Aksay, *Chem. Mater.* **2007**, *19*, 4396-4404.

[33] H. W. Kroto, J. R: Heath, S. C. O'Brien, R. F. Curl, R. E. Smalley, *Nature* **1985**, *318*, 162-163.

[34] A. Hirsch, M. Brettreich, Fullerenes: chemistry and reactions, Wiley-VCH, Weinheim, 2005.

[35] R. Taylor, J. P. Hare, A. K. Abdul-Sada AK, H. W. Kroto, *J. Chem. Soc. Chem. Commun.* **1990**, *20*, 1423-1425.

[36] P. W Fowler, A. Ceulemans, *J. Phys. Chem.* **1995**, *99*, 508-510.

[37] A. Hirsch, I. Lamparth, T. Groesser, H. R. Karfunkel, *J. Am. Chem. Soc.* **1994**, *116*, 9385-9836.

[38] A. Bianco, M. Maggini, G. Scorrano, C. Toniolo, G. Marconi, C. Villani, M. Prato, *J. Am. Chem. Soc.* **1996**, *118*, 4072-4080.

[39] M. Brettreich, A. Hirsch, *Tetrahedron Lett.* **1998**, *39*, 2731-2734.

[40] Y. Chen, R.-F. Cai, S. Chen, Z.E. Huang, *J. Phys. Chem. Solids* **2001**, *62*, 999-1001.

[41] I. Donskyi, K. Achazi, V. Wycisk, C. Böttcher, M. Adeli, *Chem. Commun.* **2016**, *52*, 4373-4376.

[42] M. Dresselhaus, G. Dresselhaus, P. Avouris, *Carbon nanotubes: synthesis, properties and applications*. 1st ed. Berlin: Springer-Verlag, **2001**.

[43] K. Balasubramanian, M. Burghard, *Anal. Bioanal. Chem.* **2006**, *385*, 452-468.

[44] D. Tasis, N. Tagmatarchis, A. Bianco, M. Prato. Chem. Rev. 2006, *106*, 1105-1136.

[45] R. Martel, *ACS Nano* **2008**, *2*, 2195-2199.

[46] Y. Wu, J. A. Phillips, H. Liu, *ACS Nano* **2008**, *2*, 2023-2028.

[47] N. W. S. Kam, Z. Liu, H. Dai, *J. Am. Chem. Soc.* **2005**, *127*, 12492-12493.

[48] R. Singh, D. Pantarotto, L. Lacerda, G. Pastorin, C. Klumpp, M. Prato, A. Bianco, K. Kostarelos, *Proc. Natl. Acad. Sci. U. S. A.* **2006**, *103*, 3357-3362.

[49] R. Krajcik, A. Jung, A. Hirsch, W. Neuhuber, O. Zolk, *Biochem. Biophys. Res. Commun.* **2008**, *369*, 595-602.

[50] M. Prato, K. Kostarelos, A. Bianco, *Acc. Chem. Res.* **2008**, *41*, 60-68.

[51] D. A. Yarotski, S. V. Kilina, A. A. Talin, S. Tretiak, O. V. Prezhdo, A. V. Balatsky, A. J. Taylor, *Nano Lett.* **2009**, *9*, 12-17.

[52] J. Chen, M. A. Hamon, H. Hu, Y. Chen, A. M. Rao, P. C. Eklund, R. C. Haddon, *Science* **1998**, *282*, 95-98.

[53] H. Hu, B. Zhao, M. E. Itkis, R. C. Haddon, *J. Phys. Chem. B* **2003**, *107*, 13838-13842.

[54] M. T. Martinez, M. A. Callejas, A. M. Benito, M. Cochet, T. Seeger, A. Anson A, J. Schreiber, C. Gordon, C. Marhic, O. Chauvet, J. L. G. Fierro, W. K. Maser, *Carbon* **2003**, *41*, 2247-2256.

[55] K. J. Ziegler, Z. Gu, H. Peng, E. L. Flor, R. H. Hauge, R. E. Smalley, *J. Am. Chem. Soc.* **2005**, *127*, 1541-1547.

[56] I. D. Rosca, F. Watari, M. Uo, T. Akasaka, *Carbon* **2005**, *43*, 3124-3131.

[57] M. Adeli, N. Mirab, M. S. Alavidjeh, Z. Sobhani, F. Atyabi, *Polymer* **2009**, *50*, 3528-3536.

[58] A. D. Maynard, P. A. Baron, M. Foley, A. A. Shvedova, E. R. Kisin, V. Castranova, *J. Toxicol. Environ. Health, Part A* **2004**, *67*, 87-107.

[59] A. Krüger, M. Ozawa, F. Kataoka, T. Fujino, Y. Suzuki, A. E. Aleksenskii, A. Ya. Vul', E. Osawa, *Carbon* **2005**, *43*, 1722-1730.

[60] R. Y. Yakovlev, A. S. Solomatin, N. B. Leonidov, I. I. Kulakova, G. V. Lisichkin, *Russ. J. Gen. Chem.* **2014**, *84*, 379-390.

[61] V. Yu. Dolmatov, *Russ. Chem. Rev.* **2001**, *70*, 607-626.

[62] J. P. L. Goncalves, A. Q. Shaikh, M Reitzig, D. A. Kovalenko, J. Michael, R. Beutner, G. Cuniberti, D. Scharnweber, J. Opitz, *Beilstein J. Org. Chem.* **2014**, *10*, 2765-2773.

[63] A. Krueger, D. Lang, *Adv. Funct. Mater.* **2012**, *22*, 890-906.

[64] A. Krueger, *J. Mater. Chem.* **2011**, *21*, 12571-12578.

[65] B. Moosa, K. Fhayli, S. Li, K. Julfakyan, A. Ezzeddine, N. M. Khashab, *J. Nanosci. Nanotechnol.* **2014**, *14*, 332-343.

[66] Y. Zhu, J. Li, W. Li, Y. Zhang, X. Yang, N. Chen, Y. Sun, Y. Zhao, C. Fan and Q. Huang, *Theranostics* **2012**, *2*, 302-312.

[67] A. M. Schrand, H. Huang, C. Carlson, J. J. Schlager, E. Omacr Sawa, S. M. Hussain, L. Dai, *J. Phys. Chem. B* **2007**, *111*, 2-7.

[68] P. W. Chen, Y. S. Ding, Q. Chen, F. L. Huang, S. R. Yun, *Diamond Relat. Mater.* **2000**, *9*, 1722-1725.

[69] E. Mironov, A. Koretz, E. Petrov, *Diamond Relat. Mater.* **2002**, *11*, 872-876.

[70] S. Bhatia, M. Dimde, R. Haag, *Med. Chem. Comm.* **2014**, *5*, 862-878.

[71] S. R. S. Ting; G. Chen, M. H. Stenzel, *Polym. Chem.* **2010**, *1*, 1392-1412.

[72] J. E. Gestwicki, C. W. Cairo, L. E. Strong,K. A. Oetjen, L. L Kiessling, *J. Am. Chem. Soc.* **2002**, *124*, 14922-14933.

[73] J. Vonnemann, S. Liese, C. Kuehne, K. Ludwig, J. Dernedde, C. Boettcher, R. R. Netz, R. Haag, *J. Am. Chem. Soc.* **2015**, *137*, 2572-2579.

[74] S. K. Choi, M. Mammen, G. M. Whitesides, *Chemistry and Biology* **1996**, *3*, 97-104.

[75] D. Bhella, *Philos. Trans. R. Soc. B* **2015**, *370*, 20140035.

[76] J. Grove, M. Marsh, *J. Cell Biol.* **2011**, *195*, 1071-1082.

[77] A. M. Krachler, H. Ham, K. Orth, *Proc. Natl. Acad. Sci. U. S. A.* **2011**, *108*, 11614-11619.

[78] J. Pizarro-Cerda, P. Cossart, *Cell.* **2006**, *124*, 715-727.

[79] D. Serrano-Gomez, A. Dominguez-Soto, J. Ancochea, J. A. Jimenez-Heffernan, J. A. Leal, A. L. Corbi, *J. Immunol.* **2004**, *173*, 5635-5643.

[80] M. J. Mendes-Giannini, C. P. Soares, J. L. da Silva, P. F. Andreotti, *FEMS Immunol. Med. Microbiol.* **2005**, *45*, 383-394.

[81] G. I. Bell, M. Dembo, P. Bongrand, *Biophys. J.* **1984**, *45*, 1051-1064.

[82] K. A. Connors, *Binding Constants: The Measurement of Molecular Complex Stability*, Wiley, New York, 1987.

[83] R.S. Kane, *Langmuir***. 2010**, *26*, 8636-8640.

[84] P. I. Kitov, D. R. Bundle, *J. Am. Chem. Soc.* **2003**, *125*, 16271-16284.

[85] M. Waldmann, R. Jirmann, K. Hoelscher, M. Wienke, F. C. Niemeyer, D. Rehders, B. Meyer, *J. Am. Chem. Soc.* **2014**, *136*, 783-788.

[86] C. Böttcher, K. Ludwig, A. Herrmann, M. van Heel, H. Stark, *FEBS Lett.* **1999**, *463*, 255-259.

[87] S. J. Watowich, J. J. Skehel, D. C. Wiley, *Structure* **1994**, *2*, 719-731.

[88] D. C. Wiley, I. A. Wilson, J. J. Skehel, *Nature* **1981**, *289*, 373-378.

[89] S. Bhatia, L. C. Camacho, R. Haag, *J. Am. Chem. Soc.* **2016**, *138*, 8954-8666.

[90] B. Michen, T. Graule, *J.of Appl. Microbiol.* **2010**, *109*, 388-397.

[91] X. Gao, K. Kim, D. Liu, *AAPS J.* **2007**, *9*, E92-E104.

[92] X. Zhang, M. Chen, R. Lam, Ḱ. X. Xu, E. Osawa, D. Ho, X. Xu, *ACS Nano* **2009**, *3*, 2609-2616.

[93] A. E. Nel, L. Mädler, D. Velegol, T. Xia, E. M. V Hoek, P. Somasundaran, F. Klaessig, V. Castranova, M. Thompson, *Nat. Mater.* **2009**, *8*, 543-557.

[94] S. Hong, P. R. Leroueil, E. K. Janus, J. L. Peters, M. Kober, *Bioconjugate Chem.* **2006**, *17*, 728-734.

[95] D. Finkelshtein, A. Werman, D. Novick, S. Barak, M. Rubinstein, S. B. D. Novick, *Proc. Natl. Acad. Sci.* **2013**, *110*, 7306-7311.

[96] M. Lüscher-Mattli, *Antivir. Chem. Chemother.* **2000**, 11, 249-259.

[97] B. Moss, *Cold Spring Harb Perspect Biol.* **2013**, *5*, a010199

[98] D. Baram-Pinto, S. Shukla, A. Gedanken, R. Sarid, *Small* **2010**, 6, 1044-1050.

[99] D. Wudunn, P. G. Spear, *J. Virol.* **1989**, *63*, 52-58.

[100] T. Cardozo, T. Kimura, S. Philpott, B. Weiser, H. Burger, S. Zolla-Pazner, *AIDS Res. Hum. Retroviruses* **2007**, *23*, 415-426.

[101] M. Moulard, H. Lortat-Jacob, I. Mondor, G. Roca, R. Wyatt, J. Sodroski, L. Zhao, W. Olson, P. D. Kwong, Q. J. Sattentau, *J. Virol.* **2000**, *74*, 1948-1960.

[102] L. Guo, N. K. Heinzinger, M. Stevenson, L. M. Schopfer, J. M. Salhany, *Antimicrob. Agents Chemother.* **1994**, *38*, 2483-2487.

[103] J. R. Bishop, M. Schuksz, J. D. Esko, *Nature* **2007**, *446*, 1030-1037.

[104] K. Forsten-Williams, C. C. Chua, M. A. Nugent, *J. Theor. Biol.* **2005**, *233*, 483-499.

[105] R. V. Iozzo, *Nature Rev. Mol. Cell Biol.* **2005**, *6*, 646-656.

[106] R. W. Mahley, Z. S. Ji, *J. Lipid Res.* **1999**, *40*, 1-16.

[107] I. Vlodavsky, O. Goldshmidt, E. Zcharia, R. Atzmon, Z. Rangini-Guatta, M. Elkin, T. Peretz, Y. Friedmann, *Semin. Cancer Biol.* **2002**, *12*, 121-129.

[108] C. Mähner, M. D. Lechner, E. Nordmeier, *Carbohydr. Res.* **2001**, *331*, 203-208.

[109] Z. Bengali, P. S. Satheshkumar, B. Moss, *Virology.* **2012**, *433*, 506-512.

[110] Z. Bengali, A. C. Townsley, B. Moss, *Virology*. **2009**, *389*, 132-140.

[111] G. C. Carter, M. Law, M. Hollinshead, G. L. Smith, *J. Gen. Virol.* **2005**, *86*, 1279-1290.

[112] C. S. Chung, J. C. Hsiao, Y. S. Chang, W. Chang, *J Virol.* **1998**, *72*, 1577-1585.

[113] J. C. Whitbeck, C. H. Foo, M. Ponce de Leon, R. J. Eisenberg, G. H. Cohen, *Virology.* **2009**, *385*, 383-391.

[114] J. Dernedde, A. Rausch, M. Weinhart, S. Enders, R. Tauber, K. Licha, M. Schirner, U. Zügel, A. von Bonin, R. Haag, *Proc. Natl. Acad. Sci. U. S. A.* **2010**, *107*, 19679-19684.

[115] W. Fischer, M. Caldero, A. Schulz, I. Andreou, M. Weber, R. Haag, *Bioconjugate. Chem.* **2010**, *21*, 1744-1752.

[116] J. Khandare, A. Mohr, M. Calderón, P. Welker, K. Licha, R. Haag, *Biomaterials* **2010**, *31*, 4268-4277.

[117] V. A. Kostyuchenko, E. X. Y. Lim, S. Zhang, G. Fibriansah, T.-S. Ng, J. S. G. Ooi, J. Shi, S.-M. Lok.

[118] A. Desfosses, E. A. Ribeiro Jr, G. Schoehn, D. Blondel, D. Guilligay, M. Jamin, R. W. H. Ruigrok, I. Gutsche, *Nat. Commun.* **2013**, *4*, 1429.

[119] K. Grünewald, P. Desai, D. C. Winkler, J. B. Heymann, D. M. Belnap, W. Baumeister, A. C. Steven, *Science* **2003**, *302*, 1396-1398.

[120] G. Andrés, R. García-Escudero, C. Simón-Mateo, E. Vinuela, *J. Virol.* **1998**, *72*, 8988-9001.

[121] G. Griffiths, N. Roos, S. Schleich, J. K. Locker, *J. Virol.* **2001**, *75*, 11056-11070.

[122] E. E. H. Tran, J. A. Simmons, A. Bartesaghi, C. J. Shoemaker, E. Nelson, J. M. White, S. Subramaniam, *J. Virol.* **2014**, *88*, 10958-10962.

[123] S. Stankovich, D. A. Dikin, G. H. Dommett, K. M. Kohlhaas, E. J. Zimney, E. A. Stach, R. D. Piner, S. T. Nguyen, R. S. Ruoff, *Nature* **2006**, *442*, 282-286.

[124] E. Lim, G. Tu, E. Schwartz, J. J. L. M. Cornelissen, A. E. Rowan, R. J. M. Nolte, W. T. S. Huck, *Macromolecules* **2008**, *41*, 1945-1951.

[125] L. Zhao, T. Takimoto, M. Ito, N. Kitagawa, T. Kimura, N. Komatsu, Angew. Chem. Int. Ed. 2011, *50*, 1388-1392.

[126] M. Terrones, *ACS Nano* **2010**, *4*, 1775-1781.

[127] A. Krueger, Y. Liang, G. Jarre, J. Stegk, *J. Mater. Chem.* **2006**, *16*, 2322-2328.

[128] E. J. Vandenberg, *J. Polym. Sci., Part A: Polym. Chem.* **1985**, *23*, 915-949.

[129] M. E. R. Weiss, *Dissertation "A kinetic model of the anionic ring-opening polymerization of glycidol"* **2012**, 18-19, Freie Universität Berlin.

[130] H. Yang, C. Shan, F. Li, D. Han, Q. Zhang, L. Niu, *Chem. Commun.* **2009**, *26*, 3880-3882.

[131] H.-X.Wang, K.-G. Zhou, Y.-L. Xie, J. Zeng, N.-N. Chai, J. Li, H.-L. Zhang, *Chem. Commun.* **2011**, *47*, 5747-5749.

[132] Z.Qi, P. Bharate, C. H. Lai, B. Ziem, C. Böttcher, A. Schulz, F. Beckert, B. Hatting, R. Mülhaupt, P. H. Seeberger, R. Haag, *Nano Lett.* **2015**, *15*, 6051-6057.

[133] J. R. Lomeda, C. D. Doyle, D. V. Kosynkin, W.-F. Hwang, J. M. Tour, *J. Am. Chem. Soc.* **2008**, *130*, 16201-16206.

[134] M. Fang, K. Wang, H. Lu, Y. Yang, S. Nutt, *J. Mater. Chem.* **2010**, *20*, 1982-1992.

[135] M. Prato, C. Li, F. Wudl, *J. Am. Chem. Soc.* **1993**, *115*, 1148-1150.

[136] C. Gao, H. He, L. Zhou, X. Zheng, Y. Zhang, *Chem. Mater.* **2009**, *21*, 360-370.

[137] S. Eigler, A. Hirsch, *Angew. Chem. Int. Ed. Engl.* **2014**, *53*, 7720-7738.

[138] A. Hirsch, J. M. Englert, F. Hauke,(2013) *Acc. Chem. Res.* **2013**, *46*, 87-96.

[139] Y. Cao, S. Osuna, Y. Liang, R. C. Haddon, K. N. Houk, *J. Am. Chem. Soc.* **2013**, *135*, 17643-17649.

[140] P. P. Brisebois, C. Kuss, S. B. Schougaard, R. Izquierdo, M. Siaj, *Chem. Eur. J.* **2016**, *22*, 5849-5852.

[141] Y. Xu, Z. Liu, X. Zhang, Y. Wang, J. Tian, Y. Huang, Y. Ma, X. Zhang, Y. Chen, *Adv. Mater.* **2009**, *21*, 1275-1279.

[142] Z. B. Liu, Y. F. Xu, X. Y. Zhang, X. L. Zhang, Y. S. Chen, J. G. Tian, *J. Phys. Chem. B* **2009**, *113*, 9681-9686.

[143] X. Zhang, Y. Huang, Y. Wang, Y. Ma, Z. Liu, Y. Chen, *Carbon* **2009**, *47*, 334-337.

[144] L. J. Hughes, J. Goldstein, J. Pohl, J. W. Hooper, R. Lee Pitts,M. B. Townsend, D. Bagarozzi, I. K. Damon, K. L. Karem, *Virology* **2014**, *464-465*, 264-273.

[145] B. Moss, *Viruses* **2012**, *4*, 688-707.

[146] M. Cyrklaff, C. Risco, J.J Ferández, M. V. Jiménez, M. Estéban, W. Baumeister, J. L. Carrascosa, *Proc. Natl. Acad. Sci. U.S.A.* **2005**, *102*, 2772-2777.

[147] G. Kochan, D. Escors, J. M. González, J. M. Casasnovas, J. M., M. Estéban, *Cell. Microbiol.* **2008**, *10*, 149-164.

[148] C.-L. Lin, C.-S. Chung, H. G. Heine, W. Chang, *J. Virol.* **2000**, *74*, 3353-3365.

[149] J. F. Rodriguez, E. Paez, M. Esteban, J. Virol. 1987, *61*, 395-404.

[150] G. Appleyard, A. J. Hapel, E. A. Boulter, *J. Gen. Virol.* **1971**, *13*, 9-17.

[151] L. G. Payne, E. Norrby, *J. Gen. Virol.* **1976**, *32*, 63-72.

[152] P. E. Pellet, B. Roizman, "The family herpesviridae: a brief introduction," in Fields Virology, D. M. Knipe and P. M. Howley, Eds., pp. 2479-2499, Lippincott Williams & Wilkins, Philadelphia, Pa, USA, 2007.

[153] D. M. Koelle, L. Corey, *Annu. Rev. Med.* **2008**, *59*, 381-395.

[154] S. E. Vleck, S. L. Oliver, J. J. Brady, H. M. Blau, J. Rajamani, M. H. Sommer, A. M. Arvin, *Proc. Natl. Acad. Sci. U.S.A.* **2011**, *108*, 18412-18417.

[155] H. G. Burke, E. E. Heldwein, *PLoS Pathog.* **2015**, *11*, e1005227

[156] Z. H. Zhou, M. Dougherty, J. Jakana, J. He, F. J. Rixon, W. Chiu, *Science* **2000**, *288*, 877-880.

[157] J. C. Brown, W. W. Newcomb, *Curr. Opin. Virol.* **2011**, *1*, 142-149.

[158] S. Laquerre, R. Argnani, D. B. Anderson, S. Zucchini, R. Manservigi, J. C. Glorioso, *J. Virol.* **1998**, *72*, 6119-6130.

[159] K. Mardberg, E. Trybala, J. C. Glorioso, T. Bergström, *J. Gen. Virol.* **2001**, *82*, 1941-1950.

[160] G. Ma, W. Azab, N. Osterrieder, *Vet. Microbiol.* **2013**, *167*, 123-134.

[161] W. Azab, K. Tsujimura, K. Maeda, K. Kobayashi, Y. M. Mohamed, K. Kato, T. Matsumura, H. Akashi, *Virus. Res.* **2010**, *151*, 1-9.

[162] G. Campadelli-Fiume, L. Menotti, *Cambridge University Press* **2007**, *7*, 93-111.

[163] N. Osterrieder, *Virus. Res.* **1999**, *59*, 165-177.

[164] P. G. Spear, *Cell. Microbiol.* **2004**, *6*, 401-410.

[165] R. J. Whitley, B. Roizman, *Lancet.* **2001**, 357, 1513-1518.

[166] L. K. Dixon, D. A. Chapman, C. L. Netherton, C. Upton, *Virus. Res.* **2013**, *173*, 3-14.

[167] G. Andrés, C. Simón-Mateo, E. Vinuela, *J. Virol.* **1997,** *71*, 2331-2341.

[168] J. L. Carrascosa, J. M. Carazo, A. L. Carrascosa, N. García, A. Santisteban, E. Vinuela, *Virology.* **1984**; *132*, 160-172.

[169] E. G. Sánchez, A. Quintas, D. Pérez-Núnez, M. Nogal, S. Barroso, Á. L. Carrascosa, Y. Revilla, *PloS. Pathoq.* **2012**, *8*, e1002754.

[170] H. Zakaryan, Y. Revilla, *Vet. Microbiol* **2016**, *185*, 15-19.

[171] B.Ziem, H. Thien, K. Achazi, C. Yue, D. Stern, K. Silberreis, M. F. Gholami, F. Beckert, D. Gröger, R. Mülhaupt, J. P. Rabe, A. Nitsche, R. Haag, *Adv. Healthc. Mater*. **2016**, doi/10.1002/adhm.201600812

8. Appendix

8.1 List of Abbreviation

α	cooperativity factor
β	enhancement factor
ΔG	binding affinity
ΔH	enthalpic change
ΔS	entropic change
0D	zero-dimensional
1D	one-dimensional
2D	two-dimensional
3D	three-dimensional
ASFV	African swine fever virus
CMV	cytomegalovirus
CNT	carbon nanotubes
CPXV	cowpox virus
CVD	chemical vapor deposition
DNA	deoxyribonucleic acid
DoS	degree of sulfation
dPGS	dendritic polyglycerol sulfate
ECM	extracellular matrix
EEV	extracellular enveloped virion
EHV-1	equine herpesvirus type-1
FTIR	Fourier transform infrared spectroscopy
GO	graphite oxide
gp	glycoprotein
H_2SO_4	sulfuric acid
HIV	human immunodeficiency virus
HIV-1	human immunodeficiency virus type-1
HNO_3	nitric acid
HS	heparan sulfate
HSPGs	heparan sulfate proteoglycans
HSV	herpes simplex virus
HSV-1	herpes simplex virus type-1

HSV-2	herpes simplex virus type-2
IMV	intracellular mature virion
K	binding constant
KO*t*Bu	potassium tert-butoxide
lPGS	linear polyglycerol sulfate
MPXV	monkeypox virus
N	monovalent binding events
N_2	nitrogen gas
ND	nanodiamond
PG	polyglycerol
PGS	polyglycerol sulfate
Prions	proteinaceous infectious particles
PRNT	plaque reduction and neutralization tests
PrV	pseudorabies virus
ROMB	ring-opening multibranching
siRNA	small interfering ribonucleic acid
SO_3	sulfur trioxide
T	temperature
TRGO	thermally reduced graphene oxide
V	variable loop
VACV	vaccinia virus
VARV	variola virus
VSV	vesicular stomatitis virus
VZV	varizella zoster virus

8.2 Publications, patent applications, and poster presentations

B.Ziem, H. Thien, K. Achazi, C. Yue, D. Stern, K. Silberreis, M. F. Gholami, F. Beckert, D. Gröger, R. Mülhaupt, J. P. Rabe, A. Nitsche, R. Haag, “Highly Efficient Multivalent 2D Nanosystems for Inhibition of Orthopoxvirus Particles” *Adv. Healthcare Mater*. **2016**, doi/10.1002/adhm.201600812

M. C. Lukowiak, **B. Ziem**, K. Achazi, G. Gunkel-Grabole, C. S. Popeney, B. N. S. Thota, C. Böttcher, A. Krueger, Z. Guan and R. Haag, " *Carbon-based cores with polyglycerol shells – The importance of core flexibility for encapsulation of hydrophobic guests" J. Mater. Chem. B,* **2015**, 3, 719-722.

Z. Qi, P. Bharate, C.-H. Lai, **B. Ziem**, C. Böttcher, A. Schulz, F. Beckert, B. Hatting, R. Mülhaupt, P. H. Seeberger and R. Haag, " *Multivalency at Interfaces: Supramolecular Carbohydrate-Functionalized Graphene Derivatives for Bacterial Capture, Release, and Disinfection" Nano Lett.* **2015**, *15*, 6051–6057.

K. Neuthe, H. Brandt, A. Hinsch, C. C. Tzschucke, W. Veurman, **B. Ziem**, and R. Haag, *"Thiocyanate-Free versus Thiocyanate-Containing Dyes for TiO2-Based Dye-Sensitized Solar Cells" ChemElectroChem*, **2014**, *1* (10), 1656–1661.

K. Neuthe, F. Bittner, F. Stiemke, **B. Ziem**, J. Du, M. Zellner, M. Wark, T. Schubert, R. Haag, "*Phosphonic acid anchored ruthenium complexes for ZnO-based dye-sensitized solar cells" Dyes and Pigments*, **2014**, *104*, 24-33.

E. Fleige, **B. Ziem**, M. Grabolle, R. Haag, U. Resch-Genger, "A*ggregation phenomena of host and guest upon the loading of dendritic core-multishell nanoparticles with salvatochromic dyes" Macromolecules* **2012**, 45, 9452−9459.

R. Haag, **B. Ziem**, A. Nitsche, Deutsche Patentanmeldung **2015**, DE-Prio-Anmeldung-Nr. 10 2015 206 814.5, Internationale Patentanmeldung **2016**, WO 2016/166316 A1, *Graphene derivative and methods for manufacturing the same*.

M. Adeli, R. Haag, **B. Ziem**, Internationale Patentanmeldung **2014**, WO 2016 050351 A1, *Controlled functionalization of carbon based materials.*

B. Ziem, Z. Qi, P. Bharate, H. Thien, F. Beckert, A. Nitsche, R. Mülhaupt, P. H. Seeberger, R. Haag; "Multivalent 2D-hybrid architectures for pathogen interaction" Macromolecular Colloquium, Freiburg, Germany, 2016.

8.3. Curriculum Vitae

Der Lebenslauf ist aus Gründen des Datenschutzes nicht enthalten.